

# Supplementary Information

## Antimalarial NADPH-Consuming Redox-Cyclers as Superior G6PD Deficiency Copycats

Max Bielitz, <sup>1</sup> Didier Belorgey, <sup>1</sup> Katharina Ehrhardt, <sup>1,2</sup> Laure Johann, <sup>1,#</sup> Don Antoine Lanfranchi, <sup>1</sup> Valentina Gallo, <sup>3</sup> Evelin Schwarzer, <sup>3</sup> Franziska Mohring, <sup>4</sup> Esther Jortzik, <sup>4</sup> David L. Williams, <sup>5</sup> Katja Becker, <sup>4</sup> Paolo Arese, <sup>3</sup> Mourad Elhabiri, <sup>1</sup> Elisabeth Davioud-Charvet <sup>1,\*</sup>

<sup>1</sup>UMR 7509 CNRS-University of Strasbourg, European School of Chemistry, Polymers and Materials (ECPM), Centre National de la Recherche Scientifique and University of Strasbourg, 25, rue Becquerel, F-67087 Strasbourg, France,

<sup>2</sup> Department of Infectiology, University of Heidelberg, Im Neuenheimer Feld 324, 69120 Heidelberg, Germany,

<sup>3</sup> Department of Oncology, University of Torino Medical School, Via Santena 5 bis, I-10126 Torino, Italy,

<sup>4</sup> Biochemistry and Molecular Biology, Interdisciplinary Research Center (IFZ), Justus Liebig University of Giessen, Heinrich-Buff-Ring 26-32, D-35392 Giessen, Germany,

<sup>5</sup> Department of Immunology/Microbiology, Rush University Medical Centre, 1735 West Harrison Street, Chicago, IL 60612, USA.

# Present adress: DSM Nutritional Products, Site Aesch, Dornacherstrasse 112, CH-4147 Aesch, Switzerland.

\*Corresponding author: Elisabeth Davioud-Charvet, UMR 7509 CNRS-University of Strasbourg, European School of Chemistry, Polymers and Materials (ECPM), 25, rue Becquerel, F-67087 Strasbourg, France. Tel: +33 3 68 85 26 20, Fax: +33 3 68 85 27 42, e-mail: elisabeth.davioud@unistra.fr

## Material and methods

Table of Content, Abbreviations	S1-S2
Definitions and abbreviations of the haem-containing compounds cited in this work	S3
Synthesis, General methods, General procedure 1	S4
(1,4-dimethoxy-3-methylnaphthalen-2-yl)(2-fluoro-4-(trifluoromethyl)phenyl)methanone ( <b>5c</b> )	S4
(1,4-dimethoxy-3-methylnaphthalen-2-yl)(2-fluoro-3-(trifluoromethyl)phenyl)methanone ( <b>5i</b> )	S4-S5
General procedure 2	S5
(2-fluoro-4-(trifluoromethyl)phenyl)(1-hydroxy-4-methoxy-3-methylnaphthalen-2-yl)methanone ( <b>6c</b> )	S5
(2-fluoro-3-(trifluoromethyl)phenyl)(1-hydroxy-4-methoxy-3-methylnaphthalen-2-yl)methanone ( <b>6i</b> )	S5-S6
General procedure 3	S6
5-methoxy-6-methyl-10-(trifluoromethyl)-7H-benzo[c]xanthen-7-one ( <b>7c</b> )	S6
5-methoxy-6-methyl-11-(trifluoromethyl)-7H-benzo[c]xanthen-7-one ( <b>7i</b> )	S6
(1,4-dihydroxy-3-methylnaphthalen-2-yl)(2-fluoro-4-(trifluoromethyl)phenyl)methanone ( <b>3c*</b> )	S6-S7
5-hydroxy-6-methyl-10-(trifluoromethyl)-7H-benzo[c]xanthen-7-one ( <b>4c</b> )	S7
2-[(4-(trifluoromethyl)phenyl)carbonyl]-4-(methoxymethoxy)-3-methylnaphthalen-1-ol ( <b>3c-MOM</b> )	S7
Physico-Biochemical Studies, Materials and Methods	S8

Electrospray Mass Spectrometric Measurements, Electrochemistry	S8
MetHb reduction coupled assay with GR/NADPH	S9
Continuous metHb redox assay in the presence of the GR/NADPH system	S9
Procedure for ferrylHb determination via sulfHb	S9
Parasitology and cell biology studies, Chemicals	S10
<i>P. falciparum</i> strains and cultures, Growth inhibition assays	S10
<i>In vitro</i> drug interaction studies	S10-S11
<i>In vitro</i> interaction of the lead parent benzylMD <b>1c</b> with the hGrx1-roGFP2 protein	S11
Imaging of the glutathione redox state in <i>Plasmodium</i> after benzylMD <b>1c</b> treatment	S11
Cultivation and separation of ring-parasitized RBC and control non-parasitized RBC, treated or not with the lead parent benzylMD <b>1c</b> and phenylhydrazine	S12
Quantification of membrane-bound haemichromes in ghosts prepared from non-parasitized and ring-parasitized RBCs, and from non-parasitized G6PD-deficient	S12
<b>Figure S1.</b> Three-step synthetic route to benzoxanthenes <b>4c</b> (LJ144, DAL105) and <b>7c</b> , <b>7i-7j</b> and structure of the benzoylMD <b>3c-MOM</b> .	S13
<b>Figure S2.</b> Cyclic voltammograms and square wave differential pulse voltammograms of menadione, benzylMD <b>1c</b> , benzoylMD <b>2c</b> , benzoxanthone <b>4c</b> , and the methoxylated benzoxanthone <b>7i</b>	S14
<b>Figure S3.</b> Stability of the benzoxanthone <b>4c</b> in aqueous buffers (a) at pH 7.4 and (b) at pH 5.2	S15
<b>Figure S4.</b> Spectrophotometric titration of haem by benzylMD <b>1c</b> , benzoylMD <b>2c</b> , reduced benzoylMD <b>3c*</b> , benzoxanthone <b>4c</b> , and chloroquine ( <b>CQ</b> ), and electronic spectra of haem, of the free drugs, and of their corresponding FeIIIPPIX.drug complexes	S16-S17
<b>Figure S5.</b> Inhibition of $\beta$ -haematin crystallization by benzoylMD <b>2c</b> , reduced benzoylMD <b>3c*</b> , measured by UV-visible absorption spectrophotometry using pyridine as reporting reagent	S18
<b>Figure S6.</b> UV-visible absorption spectra recorded as a function of time in the coupled assay in the presence of the hGR/NADPH system	S19
<b>Figure S7.</b> Controls showing the essential requirement of benzoylMD <b>2c</b> in the NADPH-dependent GR-mediated metHb reduction	S20-S21
<b>Figure S8.</b> (a) UV-visible absorption spectra recorded as a function of time showing the metHb redox cycling in the presence of benzoylMD <b>2c</b>	S22-S23
<b>Figure S9.</b> MetHb stability in aqueous buffer	S24
<b>Figure S10.</b> <i>In vitro</i> interaction of hGrx1-roGFP2 protein with the lead benzylMD <b>1c</b>	S25
NMR spectra of (1,4-dimethoxy-3-methylnaphthalen-2-yl)(2-fluoro-4-(trifluoromethyl)phenyl)methanone ( <b>5c</b> )	S26
NMR spectra of (1,4-dimethoxy-3-methylnaphthalen-2-yl)(2-fluoro-3-(trifluoromethyl)phenyl)methanone ( <b>5i</b> )	S27
NMR spectra of (2-fluoro-4-(trifluoromethyl)phenyl)(1-hydroxy-4-methoxy-3-methylnaphthalen-2-yl)methanone ( <b>6c</b> )	S28
NMR spectra of (2-fluoro-3-(trifluoromethyl)phenyl)(1-hydroxy-4-methoxy-3-methylnaphthalen-2-yl)methanone ( <b>6i</b> )	S29
NMR spectra of 5-methoxy-6-methyl-10-(trifluoromethyl)-7H-benzo[c]xanthen-7-one ( <b>7c</b> )	S30-S31
NMR spectra of 5-methoxy-6-methyl-11-(trifluoromethyl)-7H-benzo[c]xanthen-7-one ( <b>7i</b> )	S32-S33
NMR spectra of (1,4-dihydroxy-3-methylnaphthalen-2-yl)(2-fluoro-4-(trifluoromethyl)phenyl)methanone ( <b>3c*</b> )	S34
NMR spectra of 5-hydroxy-6-methyl-10-(trifluoromethyl)-7H-benzo[c]xanthen-7-one ( <b>4c</b> )	S35-S36
NMR spectra of 2-[(4-(trifluoromethyl)phenyl)carbonyl]-4-(methoxymethoxy)-3-methylnaphthalen-1-ol ( <b>3c-MOM</b> )	S37

## Abbreviations

$\epsilon$ , molar absorption coefficient; benzylMD, 3-[substituted-benzyl]-menadione; benzoylMD, 3-[substituted-benzoyl]-menadione; benzoxanthone, benzo[c]xanthen-7-one;  $\lambda$ , wavelength; CID, collision induced dissociation; DCM, dichloromethane; DMSO, dimethylsulfoxide; DV<sub>50</sub>, dissociation voltage at 50%; EDTA, ethylenediaminetetraacetic acid; EI-MS, electron impact mass spectrometry; EtOAc, ethyl acetate; Fe<sup>III</sup>PPIX, ferriprotoporphyrin or haem; Fe<sup>III</sup>(OH)PPIX, ferriprotoporphyrin monohydroxide or haematin; Fe<sup>III</sup>PPIXCl, ferriprotoporphyrin chloride or haemin; Hb(Fe<sup>II</sup>), haemoglobin subunit; HEPES, *N*-2-hydroxyethylpiperazine-*N'*-2-ethanesulfonic acid; hGR, human glutathione reductase;  $K_A$ , association constant;  $K_D$ , dissociation constant;  $K_{Dim}$ , dimerization constant; M, molar; MeOH, methanol; metHb(Fe<sup>III</sup>), methaemoglobin subunit; NADPH, reduced form of nicotinamide adenine dinucleotide phosphate; ppm, parts per million; oxyHb(Fe<sup>II</sup>), haemoglobin

subunit with O<sub>2</sub> molecule coordinated on iron<sup>II</sup>; Rf, retention factor; THF, tetrahydrofuran; TLC, thin layer chromatography; TFA, trifluoroacetic acid; tot, total; UV-vis, Ultraviolet/visible (spectroscopy).

**Definitions and abbreviations** of the haem-containing compounds cited in this work.

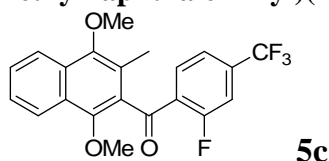
<b>Haem compound</b>	<b>Abbreviation</b>	<b>Definition</b>
Haem	Haem <b>Fe<sup>III</sup> PPIX</b>	Prosthetic group that consists of an iron atom contained in the center of a heterocyclic porphyrin ring, namely the protoporphyrin IX. It corresponds to the active protein-free unit of haemoglobin molecule.
Haematin	Haematin	Haem containing a water or and hydroxide molecule axially bound in the fifth position of the iron(III) porphyrinic system.
β-haematin	β-haematin	Synthetic haematin crystal standing for haemozoin pigment equivalent
Haemozoin	H <sub>z</sub>	Disposal pigment – biocrystals which result from self-association of Fe <sup>III</sup> protoporphyrin IX - formed during the digestion of methaemoglobin in several blood-feeding parasites (the <b>Fe<sup>III</sup> PPIX</b> are held together mainly through π-π and μ-Pr interactions).
Haemoglobin (Fe <sup>II</sup> )	Hb	Oxygen-carrying Fe <sup>II</sup> haemoprotein of erythrocytes made up of four different polypeptide globin chains that contain between 141 and 146 amino acids and a <b>Fe<sup>II</sup> PPIX</b> active site.
Methaemoglobin	metHb	Haematogenous pigment formed from haemoglobin by oxidation of the iron atom from the ferrous to the ferric state. A small amount is found in the blood normally, but injury or toxic agents convert a larger proportion of haemoglobin into methaemoglobin, which does not function as an oxygen carrier.
Ferrylhaemoglobin (Fe <sup>IV</sup> )	ferrylHb	Oxidation product of hemoglobin following hydrogen peroxide treatment. Oxidation of the iron atom from the ferrous or ferric to the ferryl states. Ferryl iron is reactive and unstable.
Haemichrome	Haemichrome	Haemichromes are low-spin Fe <sup>III</sup> species closely related to methaemoglobin (metHb). Haemichromes mainly result from denaturation processes of haemoglobin (Hb) and are characterized by the strong axial binding of two histidine residues to the ferric center following displacement of the dioxygen. Haemichromes are considered as markers of the RBC's senescence.

## Synthesis

**General methods:** Melting points were determined with a Büchi Melting Point B-540 apparatus.  $^1\text{H}$  NMR and  $^{13}\text{C}$  NMR spectra were recorded on Bruker ARX 250, Bruker DRX 300, or Bruker DRX 500 spectrometers by using  $\text{CDCl}_3$  if not otherwise indicated. Chemical shifts ( $\delta$ ) are expressed in ppm relative to TMS. Multiplicity is indicated as s (singlet), d (doublet), t (triplet), m (multiplet), bs (broad singlet), and cm (centered multiplet).  $\text{H}_{\text{ar}}$  stands for an aromatic proton in  $^1\text{H}$  NMR.  $\text{C}_q$  indicates a quaternary carbon in the  $^{13}\text{C}$  NMR assignment.  $J$  values are given in Hz.  $^{19}\text{F}$  NMR was performed using 1,2-difluorobenzene as external standard ( $\delta = -139.0$  ppm). Electron Impact (EI) mass spectra were recorded at 70 eV on Jeol JMS-700 and Finnigan TSQ 700 spectrometers at the Department of Organic Chemistry at the Ruprecht Karls University, Heidelberg. Elemental analyses were carried out in the Microanalysis Laboratory of the Faculty of Chemistry at the Ruprecht Karls University, Heidelberg. Analytical thin layer chromatography (TLC) was performed on pre-coated silica gel plates Polygram<sup>®</sup> SIL G/UV254 from Machery-Nagel, and silica gel G60 from Macherey-Nagel (230-400 mesh) was used for flash column chromatography.

**General procedure 1:** The bromonaphthalene (1.0 equiv.) was placed in an argon-flushed flask. Dry THF was added, and the mixture was cooled to  $-78$  °C. BuLi (1.1 equiv.) was added dropwise, and the mixture was stirred for 10 min at  $-78$  °C. Then, the benzoyl chloride (1.1 equiv.) was added under stirring, and the reaction mixture was stirred at  $-78$  °C for 30 min. The reaction mixture was then allowed to warm to RT. The mixture was poured into a 20 mL 1:1 mixture of diluted HCl : saturated NaCl and it was extracted twice with 20 mL  $\text{Et}_2\text{O}$ . The organic phase was dried over  $\text{MgSO}_4$  and evaporated. The resulting oil was purified through flash chromatography.

### (1,4-dimethoxy-3-methylnaphthalen-2-yl)(2-fluoro-4-(trifluoromethyl)phenyl)methanone (5c).



Yellow oil

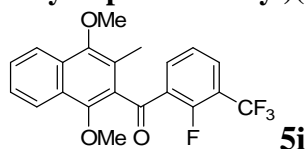
Chemical formula:  $\text{C}_{21}\text{H}_{16}\text{F}_4\text{O}_3$

Molecular weight:  $392.34 \text{ g}\cdot\text{mol}^{-1}$

Yield = 42%

2-bromo-1,4-dimethoxy-3-methylnaphthalene (300 mg, 1.07 mmol) and commercially available 2-fluoro-4-trifluoromethyl-benzoyl chloride (265 mg, 1.17 mmol) were treated according to general procedure 1. The resulting yellow oil was purified through flash chromatography (cyclohexane:EtOAc 10:1). The product **5c** was obtained as yellow oil (175 mg, 0.45 mmol, 42%). TLC (cyclohexane:EtOAc, 10:1 v/v):  $R_f = 0.50$ ;  $^1\text{H}$  NMR (300 MHz,  $\text{CDCl}_3$ ):  $\delta = 8.13$ - $8.15$  (cm, 1H),  $8.02$ - $8.05$  (cm, 1H),  $7.86$ - $7.91$  (cm, 1H),  $7.48$ - $7.62$  (cm, 3H),  $7.38$ - $7.41$  (cm, 1H),  $3.92$  (s, 3H, OCH<sub>3</sub>),  $3.79$  (s, 3H, OCH<sub>3</sub>),  $2.33$  (s, 3H, CH<sub>3</sub>);  $^{13}\text{C}$  NMR (75 MHz,  $\text{CDCl}_3$ ):  $\delta = 193.38$  (C=O),  $162.99$  (d,  $^1J_{\text{CF}} = 270$  Hz,  $\text{C}_q$ -F),  $159.53$  ( $\text{C}_q$ ),  $136.14$  ( $\text{C}_q$ ),  $132.04$  ( $\text{CH}_{\text{ar}}$ ),  $131.55$  ( $\text{C}_q$ ),  $129.95$  ( $\text{C}_q$ ),  $129.82$  ( $\text{C}_q$ ),  $127.55$  ( $\text{CH}_{\text{ar}}$ ),  $127.34$  ( $\text{C}_q$ ),  $127.01$  (q,  $^1J_{\text{CF}} = 259$  Hz,  $\text{CF}_3$ ),  $126.16$  ( $\text{CH}_{\text{ar}}$ ),  $124.54$  ( $\text{C}_q$ ),  $123.36$  ( $\text{C}_q$ ),  $122.65$  ( $\text{CH}_{\text{ar}}$ ),  $122.52$  ( $\text{CH}_{\text{ar}}$ ),  $121.19$  ( $\text{CH}_{\text{ar}}$ ),  $114.58$  ( $\text{CH}_{\text{ar}}$ ),  $63.58$  (OCH<sub>3</sub>),  $61.55$  (OCH<sub>3</sub>),  $12.74$  (CH<sub>3</sub>);  $^{19}\text{F}$  NMR (282 MHz,  $\text{CDCl}_3$ ):  $\delta = -63.29$  (s,  $\text{CF}_3$ ),  $-110.02$  (dd,  $^3J_{\text{HF}} = 10$  Hz,  $^4J_{\text{HF}} = 7$  Hz, F); EI-MS (70 eV,  $m/z$  (%)):  $392.1$  ( $[\text{M}^+]$ , 100),  $377.0$  (57),  $362.0$  (50). ESI positive-HRMS  $\text{C}_{21}\text{H}_{16}\text{F}_4\text{Na}_1\text{O}_3$   $m/z$ : found  $415.0904$ , calcd  $415.0928$ .

### (1,4-dimethoxy-3-methylnaphthalen-2-yl)(2-fluoro-3-(trifluoromethyl)phenyl)methanone (5i).



Yellow oil

Chemical formula:  $\text{C}_{21}\text{H}_{16}\text{F}_4\text{O}_3$

Molecular weight:  $392.34 \text{ g}\cdot\text{mol}^{-1}$

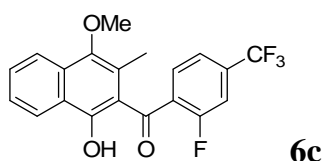
Yield = 86%

2-bromo-1,4-dimethoxy-3-methylnaphthalene (100 mg, 0.356 mmol) and commercially available 2-fluoro-3-trifluoromethyl-benzoyl chloride (90 mg, 0.392 mmol) were treated according to general procedure 1. The resulting brown oil was purified through flash chromatography (cyclohexane:EtOAc

10:1). The product **5i** was obtained as yellow oil (122 mg, 0.31 mmol, 86%). TLC (cyclohexane:EtOAc, 10:1 v/v):  $R_f = 0.35$ ;  $^1\text{H NMR}$  (300 MHz,  $\text{CDCl}_3$ ):  $\delta = 8.13\text{--}8.15$  (m, 1H), 8.03–8.05 (m, 1H), 7.92–7.98 (m, 1H), 7.79–7.83 (m, 1H), 7.50–7.62 (cm, 2H), 7.31–7.36 (m, 1H), 3.92 (s, 3H, OCH<sub>3</sub>), 3.79 (s, 3H, OCH<sub>3</sub>), 2.33 (s, 3H, CH<sub>3</sub>);  $^{13}\text{C NMR}$  (75 MHz,  $\text{CDCl}_3$ ):  $\delta = 193.18$  (C=O), 159.01 (d,  $^1J_{\text{CF}} = 269$  Hz, C<sub>q</sub>-F), 150.69 (C<sub>q</sub>), 149.83 (C<sub>q</sub>), 137.19 (CH<sub>ar</sub>), 135.05 (CH<sub>ar</sub>), 133.42 (C<sub>q</sub>), 131.63 (C<sub>q</sub>), 131.51 (CH<sub>ar</sub>), 128.50 (C<sub>q</sub>), 128.43 (q,  $^1J_{\text{CF}} = 259$  Hz, CF<sub>3</sub>), 128.38 (C<sub>q</sub>), 127.52 (CH<sub>ar</sub>), 126.13 (CH<sub>ar</sub>), 124.40 (C<sub>q</sub>), 124.18 (CH<sub>ar</sub>), 123.32 (C<sub>q</sub>), 122.62 (CH<sub>ar</sub>, d,  $J = 12.6$  Hz), 63.54 (OCH<sub>3</sub>), 61.55 (OCH<sub>3</sub>), 12.75 (CH<sub>3</sub>); EI-MS (70 eV,  $m/z$  (%)): 392.0 ([M<sup>+</sup>], 25).

**General procedure 2:** A solution of dimethoxynaphthalene (1.0 equiv.) in dry DCM was cooled to 0 °C and kept stirring for 30 min. Then, BBr<sub>3</sub> (1.0 equiv., 1 M in DCM) was added dropwise to the solution, and the reaction mixture was stirred at 0 °C for 2 h (TLC control). The reaction mixture was quenched with MeOH. Saturated NaCl was added to the mixture, which was extracted three times with DCM and twice with EtOAc. The organic layers were combined, dried over MgSO<sub>4</sub>, and evaporated.

**(2-fluoro-4-(trifluoromethyl)phenyl)(1-hydroxy-4-methoxy-3-methylnaphthalen-2-yl)methanone (6c).**



Yellow solid

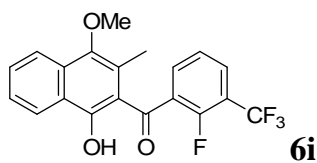
Chemical formula: C<sub>20</sub>H<sub>14</sub>F<sub>4</sub>O<sub>3</sub>

Molecular weight: 378.32 g.mol<sup>-1</sup>

Yield = 68%

(1,4-dimethoxy-3-methylnaphthalen-2-yl)(2-fluoro-4-(trifluoromethyl)phenyl)methanone **5c** (230 mg, 0.60 mmol) was used as a starting material and treated according to general procedure 2. The resulting yellow oil was purified through flash chromatography (DCM:cyclohexane 1:1). The product **6c** was obtained as a yellow solid (150 mg, 0.40 mmol, 68%), TLC (DCM:cyclohexane, 1:1 v/v):  $R_f = 0.55$ ;  $^1\text{H NMR}$  (300 MHz,  $\text{CDCl}_3$ ):  $\delta = 12.87$  (OH), 8.48–8.50 (m, 1H), 8.00–8.03 (m, 1H), 7.69–7.74 (m, 1H), 7.52–7.63 (cm, 3H), 7.43–7.46 (m, 1H), 3.82 (s, 3H, OCH<sub>3</sub>), 1.98 (s, 3H, CH<sub>3</sub>);  $^{13}\text{C NMR}$  (75 MHz,  $\text{CDCl}_3$ ):  $\delta = 195.71$  (C=O), 160.46 (d,  $^1J_{\text{CF}} = 270$  Hz, C<sub>q</sub>-F), 159.53 (C<sub>q</sub>), 133.30 (C<sub>q</sub>), 132.20 (C<sub>q</sub>), 130.35 (C<sub>q</sub>), 129.90 (C<sub>q</sub>), 128.30 (CH<sub>ar</sub>), 123.44 (C<sub>q</sub>), 123.37 (CH<sub>ar</sub>), 123.29 (CH<sub>ar</sub>), 122.72 (C<sub>q</sub>), 120.08 (q,  $^1J_{\text{CF}} = 259$  Hz, CF<sub>3</sub>), 119.79 (CH<sub>ar</sub>), 119.06 (CH<sub>ar</sub>), 118.91 (CH<sub>ar</sub>), 116.13 (C<sub>q</sub>), 113.86 (CH<sub>ar</sub>), 61.07 (OCH<sub>3</sub>), 15.48 (CH<sub>3</sub>);  $^{19}\text{F NMR}$  (282 MHz,  $\text{CDCl}_3$ ):  $\delta = -63.01$  (s, CF<sub>3</sub>), -111.93 (dd,  $^3J_{\text{HF}} = 10$  Hz,  $^4J_{\text{HF}} = 7$  Hz, F); EI-MS (70eV,  $m/z$  (%)): 378.0 ([M<sup>+</sup>], 100), 363.0 (52), 345.0 (35).

**(2-fluoro-3-(trifluoromethyl)phenyl)(1-hydroxy-4-methoxy-3-methylnaphthalen-2-yl)methanone (6i).**



Bright yellow oil

Chemical formula: C<sub>20</sub>H<sub>14</sub>F<sub>4</sub>O<sub>3</sub>

Molecular weight: 378.32 g.mol<sup>-1</sup>

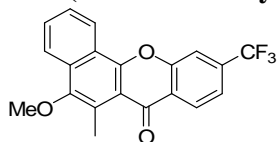
Yield = 38%

(1,4-dimethoxy-3-methylnaphthalen-2-yl)(2-fluoro-3-(trifluoromethyl)phenyl)methanone **5i** (400 mg, 1.02 mmol) was used as a starting material and treated according to general procedure 2. The resulting dark yellow oil was purified through flash chromatography (cyclohexane:EtOAc 10:1). The product was obtained as bright yellow oil (150 mg, 0.40 mmol, 38%). TLC (cyclohexane:EtOAc 10:1 v/v):  $R_f = 0.23$ ;  $^1\text{H NMR}$  (300 MHz,  $\text{CDCl}_3$ ):  $\delta = 12.80$  (OH), 8.47–8.50 (m, 1H), 8.00–8.03 (m, 1H), 7.77–7.82 (cm, 1H), 7.68–7.73 (cm, 2H), 7.52–7.57 (m, 1H), 7.36–7.41 (cm, 1H), 3.81 (s, 3H, OCH<sub>3</sub>), 1.97 (s, 3H, CH<sub>3</sub>);  $^{13}\text{C NMR}$  (75 MHz,  $\text{CDCl}_3$ ):  $\delta = 195.51$  (C=O), 159.50 (C<sub>q</sub>), 156.48 (dd,  $^1J_{\text{CF}} = 262$  Hz,  $^3J_{\text{CF}} = 6$  Hz, C<sub>q</sub>-F), 146.99 (C<sub>q</sub>), 133.47 (CH<sub>ar</sub>), 132.22 (C<sub>q</sub>), 131.56 (d,  $^2J_{\text{CqCF}} = 14$  Hz, C<sub>q</sub>), 130.87 (CH<sub>ar</sub>), 129.90 (dd,  $J = 4.5$  Hz,  $J = 1.8$  Hz, CH<sub>ar</sub>), 125.94 (CH<sub>ar</sub>), 125.01 (CH<sub>ar</sub>), 124.89 (C<sub>q</sub>), 124.64 (d,  $^3J_{\text{CHar-F}} = 4.7$  Hz, CH<sub>ar</sub>), 122.66 (C<sub>q</sub>), 122.21 (q,  $^1J_{\text{CF}} = 273$  Hz, CF<sub>3</sub>), 121.90 (CH<sub>ar</sub>), 119.33 (dd,  $^2J_{\text{CqCF}} = 33$  Hz,

C<sub>q</sub>-CF<sub>3</sub>) 116.08 (C<sub>q</sub>), 61.09 (OCH<sub>3</sub>), 15.51 (CH<sub>3</sub>); <sup>19</sup>F NMR (282 MHz, CDCl<sub>3</sub>): δ = -61.49 (d, <sup>4</sup>J<sub>FF</sub> = 13 Hz, CF<sub>3</sub>), -115.91 (<sup>4</sup>J<sub>FF</sub> = 13 Hz, <sup>4</sup>J<sub>HF</sub> = 6 Hz, F); EI-MS (70 eV, *m/z* (%)): 378.3 ([M<sup>+</sup>], 48).

**General procedure 3:** The benzophenone derivative (1.0 equiv.) and K<sub>2</sub>CO<sub>3</sub> (2.0 equiv.) were placed in a round-bottom flask. The flask was sealed under argon, and 10 mL of dry acetone was added. The reaction mixture was stirred at 50 °C for 2 h. The suspension was filtered through a pad of celite and washed with 25 mL Et<sub>2</sub>O. The filtrate was concentrated under vacuum.

**5-methoxy-6-methyl-10-(trifluoromethyl)-7H-benzo[*c*]xanthen-7-one (7c).**



**7c**

White "cotton-like" solid

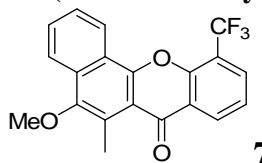
Chemical formula: C<sub>20</sub>H<sub>13</sub>F<sub>3</sub>O<sub>3</sub>

Molecular weight: 358.31 g.mol<sup>-1</sup>

Yield = 77%

(2-fluoro-4-(trifluoromethyl)phenyl)(1-hydroxy-4-methoxy-3-methylnaphthalen-2-yl)methanone **6c** (150 mg, 0.40 mmol) was used as a starting material and treated according to general procedure 3. The product **7c** was obtained as a white, cotton-like solid (110 mg, 0.31 mmol, 77%), m.p. 167-169 °C; TLC (DCM:cyclohexane, 1:1 v/v): R<sub>f</sub> = 0.37; <sup>1</sup>H NMR (300 MHz, CDCl<sub>3</sub>): δ = 8.62-8.69 (m, 1H), 8.42-8.44 (m, 1H), 8.13-8.16 (m, 1H), 7.90 (s, 1H), 7.73-7.78 (cm, 1H), 7.61-7.67 (m, 2H), 3.91 (s, 3H, OCH<sub>3</sub>), 2.93 (s, 3H, CH<sub>3</sub>); <sup>13</sup>C NMR (75 MHz, CDCl<sub>3</sub>): δ = 177.64 (C=O), 154.21 (C<sub>q</sub>), 152.02 (C<sub>q</sub>), 150.33 (C<sub>q</sub>), 135.38 (q, <sup>2</sup>J<sub>CqCF</sub> = 33 Hz, C<sub>q</sub>-CF<sub>3</sub>), 131.24 (C<sub>q</sub>), 130.26 (CH<sub>ar</sub>), 127.93 (CH<sub>ar</sub>), 126.63 (CH<sub>ar</sub>), 125.70 (C<sub>q</sub>), 125.20 (C<sub>q</sub>), 123.52 (C<sub>q</sub>), 123.25 (q, <sup>1</sup>J<sub>CF</sub> = 273 Hz, CF<sub>3</sub>), 123.17 (CH<sub>ar</sub>), 122.28 (CH<sub>ar</sub>), 120.53 (q, <sup>3</sup>J<sub>CHar-F</sub> = 4 Hz, CH<sub>ar</sub>), 117.52 (C<sub>q</sub>), 115.44 (q, <sup>3</sup>J<sub>CHar-F</sub> = 4 Hz, CH<sub>ar</sub>), 61.47 (OCH<sub>3</sub>), 14.44 (CH<sub>3</sub>); <sup>19</sup>F NMR (CDCl<sub>3</sub>, 282 MHz): δ = -62.95 (s, CF<sub>3</sub>); EI-MS (70 eV, *m/z* (%)): 358.0 ([M<sup>+</sup>], 53); analysis (calcd, found for C<sub>20</sub>H<sub>13</sub>O<sub>3</sub>F<sub>3</sub>): C (67.04, 66.64), H (3.66, 3.81). ESI positive-HRMS C<sub>20</sub>H<sub>14</sub> F<sub>3</sub>O<sub>3</sub> *m/z*: found 359.0893, calcd 359.0890.

**5-methoxy-6-methyl-11-(trifluoromethyl)-7H-benzo[*c*]xanthen-7-one (7i).**



**7i**

Light yellow "cotton-like" solid

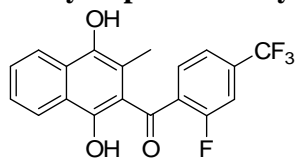
Chemical formula: C<sub>20</sub>H<sub>13</sub>F<sub>3</sub>O<sub>3</sub>

Molecular weight: 358.31 g.mol<sup>-1</sup>

Yield = 86%

(2-fluoro-3-(trifluoromethyl)phenyl)(1-hydroxy-4-methoxy-3-methylnaphthalen-2-yl)methanone **6i** (150 mg, 0.40 mmol) was used as a starting material and treated according to general procedure 3. The product **7i** obtained as a light yellow, cotton-like solid (120 mg, 0.33 mmol, 86%), m.p. 198-200 °C; <sup>1</sup>H NMR (300 MHz, CDCl<sub>3</sub>): δ = 8.64-8.67 (m, 1H), 8.53-8.57 (m, 1H), 8.17-8.19 (m, 1H), 8.02-8.05 (m, 1H), 7.76-7.81 (cm, 1H), 7.67-7.73 (cm, 1H), 7.47-7.53 (cm, 1H), 3.93 (s, 3H, OCH<sub>3</sub>), 2.97 (s, 3H, CH<sub>3</sub>); <sup>13</sup>C NMR (75 MHz, CDCl<sub>3</sub>): δ = 177.39 (C=O), 151.79 (C<sub>q</sub>), 151.51 (C<sub>q</sub>), 150.50 (C<sub>q</sub>), 131.27 (q, <sup>3</sup>J<sub>CHar-F</sub> = 4 Hz, CH<sub>ar</sub>), 131.24 (C<sub>q</sub>), 130.99 (CH<sub>ar</sub>), 130.29 (CH<sub>ar</sub>), 126.90 (CH<sub>ar</sub>), 125.55 (C<sub>q</sub>), 124.04 (C<sub>q</sub>), 123.70 (C<sub>q</sub>), 123.48 (CH<sub>ar</sub>), 123.33 (CH<sub>ar</sub>), 123.13 (q, <sup>1</sup>J<sub>CF</sub> = 273 Hz, CF<sub>3</sub>), 122.14 (CH<sub>ar</sub>), 119.08 (q, <sup>2</sup>J<sub>CqCF</sub> = 32 Hz, C<sub>q</sub>-CF<sub>3</sub>), 117.31 (C<sub>q</sub>), 61.54 (OCH<sub>3</sub>), 14.46 (CH<sub>3</sub>); <sup>19</sup>F NMR (282 MHz, CDCl<sub>3</sub>): δ = -61.31 (s, CF<sub>3</sub>); EI-MS (70 eV, *m/z* (%)): 358.0 ([M<sup>+</sup>], 60), 343.0 (100); analysis (calcd, found for C<sub>20</sub>H<sub>13</sub>O<sub>3</sub>F<sub>3</sub>): C (67.04, 66.95), H (3.66; 3.80). ESI positive-HRMS C<sub>20</sub>H<sub>14</sub> F<sub>3</sub>O<sub>3</sub> *m/z*: found 359.0912, calcd 359.0890.

**(1,4-dihydroxy-3-methylnaphthalen-2-yl)(2-fluoro-4-(trifluoromethyl)phenyl)methanone (3c\*).**



**3c\***

Bright orange crystals

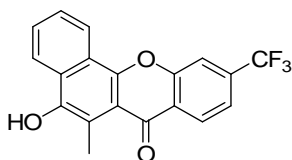
Chemical formula: C<sub>19</sub>H<sub>12</sub>F<sub>4</sub>O<sub>3</sub>

Molecular weight: 364.29 g.mol<sup>-1</sup>

Yield = 52%

(1,4-dimethoxy-3-methylnaphthalen-2-yl)(2-fluoro-4-(trifluoromethyl)phenyl)methanone **3c** (250 mg, 0.64 mmol) dissolved in 40 mL DCM was cooled to 0 °C and kept stirring for 30 min. Pure BBr<sub>3</sub> (61 μL, 0.64 mmol, 1.0 equiv.) was added dropwise to the solution, and the reaction mixture was stirred at 0 °C for 1 h. The reaction mixture was quenched with 60 mL MeOH. Saturated NaCl was added to the mixture, and it was extracted with DCM (2 x 50 mL). The organic layer was dried over MgSO<sub>4</sub> and evaporated to give 500 mg of a red-orange solid. The red-orange residue was recrystallized in 10 mL of a 10:1 cyclohexane:EtOAc mixture. The product **3c\*** was obtained as bright orange crystals (121 mg, 0.33 mmol, 52%), m.p. 104 °C (dec.), <sup>1</sup>H NMR (300 MHz, CDCl<sub>3</sub>): δ = 12.55 (s, 1H, OH), 8.46-8.49 (m, 1H), 8.06-8.09 (m, 1H), 7.69-7.74 (cm, 1H), 7.51-7.62 (cm, 3H), 7.45-7.42 (m, 1H), 4.68 (s, 1H, OH), 1.94 (s, 3H, CH<sub>3</sub>); <sup>13</sup>C NMR (75 MHz, CDCl<sub>3</sub>): δ = 194.44 (C=O), 161.87 (C<sub>q</sub>), 159.31 (C<sub>q</sub>), 147.61 (d, <sup>1</sup>J<sub>CF</sub> = 311.7 Hz, C<sub>q</sub>-F), 144.77 (C<sub>q</sub>), 143.80 (C<sub>q</sub>), 134.15 (dq, <sup>2</sup>J<sub>CqCF</sub> = 33 Hz, <sup>3</sup>J<sub>CF</sub> = 9 Hz, C<sub>q</sub>-CF<sub>3</sub>), 132.66 (CH<sub>ar</sub>), 131.88 (d, J = 10.3 Hz, CH<sub>ar</sub>), 127.92 (C<sub>q</sub>), 127.17 (CH<sub>ar</sub>), 125.44 (CH<sub>ar</sub>), 124.98 (d, <sup>2</sup>J<sub>CqCF</sub> = 23 Hz, C<sub>q</sub>), 122.84 (CH<sub>ar</sub>), 122.70 (CH<sub>ar</sub>), 122.10 (CH<sub>ar</sub>), 116.27 (C<sub>q</sub>), 114.89 (dd, <sup>2</sup>J<sub>CqCF</sub> = 25 Hz, <sup>3</sup>J<sub>CH<sub>ar</sub>-F</sub> = 4 Hz, CH<sub>ar</sub>), 13.76 (CH<sub>3</sub>); <sup>19</sup>F NMR (CDCl<sub>3</sub>, 282 MHz): δ = -63.44 (s, CF<sub>3</sub>), -111.44 (dd, <sup>3</sup>J<sub>HF</sub> = 10 Hz, <sup>4</sup>J<sub>HF</sub> = 7 Hz, F); EI-MS (70 eV, m/z (%)): 364.1 ([M<sup>+</sup>], 100); analysis (calcd, found for C<sub>19</sub>H<sub>12</sub>O<sub>3</sub>F<sub>4</sub>): C (62.64, 62.20), H (3.32, 3.08). ESI positive-HRMS C<sub>19</sub>H<sub>10</sub>F<sub>4</sub>NaO<sub>3</sub> m/z: found 385.0458, calcd 385.0468.

#### 5-hydroxy-6-methyl-10-(trifluoromethyl)-7H-benzo[c]xanthen-7-one (**4c**).



**4c**

Bright yellow solid

Chemical formula: C<sub>19</sub>H<sub>11</sub>F<sub>3</sub>O<sub>3</sub>

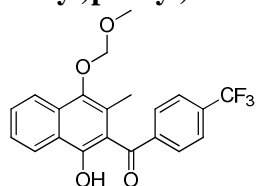
Molecular weight: 344.28 g.mol<sup>-1</sup>

Yield = 63%, Overall yield after 6 steps

from menadione: 26% (via **3c\***)

(1,4-dihydroxy-3-methylnaphthalen-2-yl)(2-fluoro-4-(trifluoromethyl)phenyl)methanone **3c\*** (100 mg, 0.275 mmol) was used as a starting material and treated according to general procedure 3. The resulting red-orange solid (90 mg) was recrystallized in 5 mL cyclohexane:EtOAc:acetone, 10:1:0.1 v/v. The product **4c** was obtained as a bright yellow solid (60 mg, 0.17 mmol, 63%), m.p. 229-231 °C, <sup>1</sup>H NMR (300 MHz, CDCl<sub>3</sub>): δ = 8.64-8.67 (m, 1H), 8.46-8.48 (m, 1H), 8.28-8.31 (m, 1H), 7.95 (s, 1H), 7.63-7.81 (m, 3H), 5.33 (s, 1H, OH), 2.96 (s, 3H, CH<sub>3</sub>), <sup>13</sup>C NMR (75 MHz, DMSO-*d*<sub>6</sub>): δ = 176.87 (C=O), 153.74 (C<sub>q</sub>), 148.96 (C<sub>q</sub>), 146.30 (C<sub>q</sub>), 133.43 (d, <sup>2</sup>J<sub>CqCF</sub> = 32 Hz, C<sub>q</sub>-CF<sub>3</sub>), 129.66 (CH<sub>ar</sub>), 128.97 (C<sub>q</sub>), 127.57 (CH<sub>ar</sub>), 126.60 (CH<sub>ar</sub>), 124.73 (C<sub>q</sub>), 123.37 (q, <sup>1</sup>J<sub>CF</sub> = 273 Hz, CF<sub>3</sub>), 122.72 (CH<sub>ar</sub>), 122.37 (C<sub>q</sub>), 122.30 (CH<sub>ar</sub>), 120.10 (q, <sup>3</sup>J<sub>CH<sub>ar</sub>-F</sub> visible, CH<sub>ar</sub>), 116.92 (C<sub>q</sub>), 115.92 (C<sub>q</sub>), 115.88 (d, J = 3.9 Hz, CH<sub>ar</sub>), 14.01 (CH<sub>3</sub>), <sup>19</sup>F NMR (CDCl<sub>3</sub>, 282 MHz): δ = -63.03 (s, CF<sub>3</sub>), EI-MS (70 eV, m/z (%)): 344.0 ([M<sup>+</sup>], 100), analysis (calcd, found for C<sub>19</sub>H<sub>11</sub>O<sub>3</sub>F<sub>3</sub>): C (66.28, 66.23), H (3.22, 3.58). ESI positive-HRMS C<sub>19</sub>H<sub>12</sub>F<sub>3</sub>O<sub>3</sub> m/z: found 345.0739, calcd 345.0733.

#### 2-[(4-(trifluoromethyl)phenyl)carbonyl]-4-(methoxymethoxy)-3-methylnaphthalen-1-ol (**3c-MOM**)



**3c-MOM**

Orange oil

Chemical formula: C<sub>21</sub>H<sub>17</sub>F<sub>3</sub>O<sub>4</sub>

Molecular weight: 408.34 g.mol<sup>-1</sup>

Overall Yield = 64% (5 steps)

The synthesis of **3c-MOM** and benzoxanthone **4c** (49% yield in 6 steps from menadione) via **3c-MOM** will be described separately, along with all related data acquired in electro- and physico-chemistry.

## Physico-Biochemical Studies

The experimental conditions related to (i) the spectrophotometric titration of haematin  $\pi$ - $\pi$  dimer by the substrates, (ii) the  $\beta$ -haematin inhibition assay, and (iii) the metHb reduction assay, are available in ref. 1.

**Materials and Methods:** Distilled water was purified by passing it through a mixed bed of ion-exchanger (Bioblock Scientific R3-83002, M3-83006) and activated carbon (Bioblock Scientific ORC-83005). DMSO (E. Merck, Uvasol, for spectroscopy or Sigma, Bioreagent, for molecular biology), acetonitrile (E. Merck Uvasol, for spectroscopy), and chloroquine (Sigma, diphosphate salt) were obtained from commercial suppliers and used without further purification. Haematin ( $\text{Fe}^{\text{III}}\text{PPIX}(\text{OH})$ ) solution was prepared from haemin equine Type III ( $\text{Fe}^{\text{III}}\text{PPIXCl}$ , Sigma-Aldrich) and 50% aqueous ammonia (ESI-MS CID experiments) vigorously stirred at room temperature (RT) for 1 h. Stock solutions (DMSO) of the substrates (**1c–4c**, CQ, AQ) for the different assays were freshly prepared in Eppendorf tubes just before the experiments. All stock solutions were prepared using an AG 245 Mettler Toledo analytical balance.

**Electrospray Mass Spectrometric Measurements:** Electrospray mass spectra of haem complexes were obtained with a Bruker Daltonics MicroTOF spectrometer (Bruker Daltonik GmbH, Bremen, Germany) equipped with an orthogonal electrospray (ESI) interface. Calibration was performed using Tuning mix (Agilent Technologies). CID experiments were performed with a capillary exit (cone voltage) ranging from 120 to 400V with 20V increments.<sup>2</sup> Stock solution of haematin ( $[\text{Fe}^{\text{III}}\text{PPIX}(\text{OH}_2)]^{3+}$  or  $[\text{Fe}^{\text{III}}\text{PPIX}(\text{OH})]^{2+}$ ) was freshly prepared from haemin (ferriprotoporphyrin chloride,  $[\text{Fe}^{\text{III}}\text{PPIX}(\text{Cl})]^{2+}$ ) just before use in 50% ammonia. Stock solution of benzoxanthone **4c** (5 mM) was prepared in  $\text{CH}_3\text{CN}$ , while chloroquine (**CQ**, 2.91 mM) and amodiaquine (**AQ**, 2.28 mM) were prepared in water. Haematin and the substrate (**4c** or **CQ** or **AQ**) were mixed together in  $\text{CH}_3\text{CN}/\text{H}_2\text{O}$  (50:50 v:v) in order to obtain equimolar concentrations of 100  $\mu\text{M}$ . Prior to analyses, the samples were further diluted at 50  $\mu\text{M}$  in  $\text{CH}_3\text{CN}/\text{H}_2\text{O}/\text{HCO}_2\text{H}$  (50:50:1 v:v:v). The sample solutions were then introduced into the spectrometer source with a syringe pump (Harvard type 55 1111: Harvard Apparatus Inc., South Natick, MA, USA) with a flow rate of 5  $\mu\text{L}\cdot\text{min}^{-1}$ .

**Electrochemistry:** Cyclic voltammetry (CV) and square wave voltammetry (SWV) experiments of menadione, benzylMD **1c**, benzoylMD **2c**, and benzoxanthenes **4c** and **7i** were performed on a Voltalab 50 potentiostat/galvanostat (Radiometer Analytical) controlled by the Voltmaster 4 electrochemical software at different scan rates and at room temperature ( $25 \pm 1$  °C). A conventional three-electrode cell (10 mL) was employed with a glassy carbon disk from spectroscopic graphite rods set into a Teflon tube ( $s = 0.071$  cm<sup>2</sup>) as a working electrode, a Pt wire as a counter electrode, and KCl (3.5 M)/Ag/AgCl reference electrode (+205 mV vs NHE).<sup>3</sup> Prior to a voltammetry experiment, the working electrode was mechanically polished with and without alumina suspension (ESCIL, 0.3  $\mu\text{m}$ ) on a silicon carbide paper (800/2400 grit) followed by sonication in Milli-Q water. The menadione, benzylMD **1c**, benzoylMD **2c**, and benzoxanthenes **4c** or **7i** solutions ( $\sim 1$  mM) were prepared with spectroscopic-grade DMSO (E. Merck, Uvasol, for spectroscopy or Sigma, Bioreagent, for molecular biology) as solvent and with 0.1 M tetrabutylammonium hexafluorophosphate ( $\text{NBu}_4\text{PF}_6$ ) as electrolyte support. All the solutions were carefully deoxygenated with argon for 30 min (Sigma Oxiclear cartridge). The electrode was installed into the voltammetric cell along with the platinum wire counter electrode and the reference. The substrates were then introduced ( $\sim 10$  mL), and the solution was again purged for 10 min with argon

<sup>1</sup> Johann, L. *et al.* A physico-biochemical study on potential redox-cyclers as antimalarial and anti-schistosomal drugs. *Curr. Pharm. Des.* **18**, 3539-3566 (2012).

<sup>2</sup> Mishra, E. *et al.* Axial imidazole binding strengths in porphyrinoid cobalt(III) complexes as studied by tandem mass spectrometry. *J. Am. Soc. Mass Spectrom.* **23**, 1428-1439 (2012).

<sup>3</sup> Sawyer, D. T., Sobkowiak, A. & Roberts, J. L. *Electrochemistry for Chemists*, 2<sup>nd</sup> Ed.; Wiley: New York, **1995**, p 192.



(Sigma Oxiclear cartridge) before the voltammetry experiment was initiated. Voltammograms were generally recorded at a sweep rate of 200 mV s<sup>-1</sup>. The redox potentials E<sub>1/2</sub> were determined from the corresponding oxidation and reduction potentials. All potential measurements were referred to a saturated calomel electrode (SCE).

**MetHb reduction coupled assay with GR/NADPH:** *hGR* and *PfGR* were purified and quantified as described previously.<sup>4,5</sup> A 1 mL solution containing metHb (8 μM final), the drug (40 μM final), NADPH (120 μM final) was incubated at 25 °C in GR buffer. *hGR* or *PfGR* was then added (100 nM final) and the reaction followed by UV-vis absorption spectrophotometry between 300 and 700 nm. Different controls showing the essential requirement of the benzoylMD **2c**, in the presence of GSH or GSSG are shown in Fig. S7.

**Continuous metHb redox assay in the presence of the GR/NADPH system:** Stock solutions of 2 mM of the drugs in DMSO were freshly prepared. Solutions of 0.8 mM metHb in water and 16 mM NADPH in water were prepared and kept at 0 °C during the experiment. In a Hellma optical cell (*l* = 0.5 cm), 878 μL of the *hGR* buffer, 40 μL of the metHb solution (0.8 mM), 20 μL of the drug solution (2 mM), and 30 μL of the NADPH solution (16 mM) were introduced at 25 °C (Lauda E200/O11 thermostat and a Huber Minichiller cooler) for 3-5 min. Then, 32 μL of the GR stock solution (12.5 μM) was added. After the redox cycling had stopped, 30 μL of a 16 mM NADPH solution was added. The reaction was monitored by UV-vis absorption spectrophotometry on a Cary 50 or Cary 300 spectrophotometer with the scanning kinetics method. A spectrum was measured every 10 min or 30 min, depending on the experiment, between 300 and 700 nm for the stated period of time. The kinetic data were processed with the Specfit program.

**Procedure for ferrylHb determination via sulfHb:** Several 1 mL samples of the metHb reduction reaction were prepared at the same time in separate Eppendorf vials and tempered at 25 °C according to the continuous metHb redox assay above. The assay was monitored every 30 min by UV-Vis spectrophotometry for 7 hours (fig. 3b and fig. S8a,c). Every hour one new sample (500 μL) was taken and transferred into a cuvette [Hellma optical cell (*l* = 1 cm)]. This cuvette was placed in another spectrophotometer and the reaction mixture was reacted with 10 μL of catalase (EC 1.11.1.6, 61 Units final as defined by Sigma) for 30 seconds to destroy excess of H<sub>2</sub>O<sub>2</sub> and then with 5 μL of aq. Na<sub>2</sub>S solution (200 mM stock solution). Spectra were recorded every min for a period of 20 min to ensure equilibration. The characteristic peak for sulfHb at 620 nm was integrated to determine its area using Origin as data processing program (**Fig. S8b**).

## Parasitology and cell biology studies

### Chemicals

ML276 or (R,Z)-*N*-((1-ethylpyrrolidin-2-yl)methyl)-2-(2-fluorobenzylidene)-3-oxo-3,4-dihydro-2*H*-benzo[*b*][1,4]thiazine-6-carboxamide) was provided by the laboratory of Pr. Katja Becker. CB83 or *N*-(4-hydroxy-1-naphthalenyl)-2,5-dimethyl-benzenesulfonamide was purchased from Interchim (Montluçon, France). The compounds diamide or *N,N,N',N'*-tetramethylazodicarboxamide, phenylhydrazine, nicotinamide, 6-aminonicotinamide, desferrioxamine (DFO) and epigallocatechin-3-gallate (EGCG) were purchased from Sigma-Aldrich. Stock solutions of compounds were prepared in

<sup>4</sup> Nordhoff A., Bucheler U. S., Werner D. & Schirmer R. H. Folding of the four domains and dimerization are impaired by the Gly446→Glu exchange in human glutathione reductase. Implications for the design of antiparasitic drugs. *Biochemistry* **32**: 4060-4066 (1993).

<sup>5</sup> Färber, P. M., Arscott, L. D., Williams, C. H., Becker, K. & Schirmer, R. H. Recombinant *Plasmodium falciparum* glutathione reductase is inhibited by the antimalarial dye methylene blue. *FEBS Lett.* **422**, 311-314 (1998).

pure water (nicotinamide, DFO, EGCG) or in DMSO (**1c**, P\_TM101 (or compound 7a in ref. 6), **4c**, ML276, CB83 and 6-aminonicotinamide). All stock solutions were stored in aliquots at -20 °C.

***P. falciparum* strains and cultures:** *In vitro* studies using living *P. falciparum* blood stage parasites were performed in three different laboratories [laboratory A = Department of Infectiology, University of Heidelberg, Germany; laboratory B = Museum National d'Histoire Naturelle, Paris, France; laboratory C = Interdisciplinary Research Centre, Justus Liebig Giessen University, Germany], herein after referred to as laboratory A, B or C. Cultures of *P. falciparum* strain 3D7 (chloroquine sensitive) or strain Dd2 (chloroquine resistant) were maintained according to standard protocols<sup>7</sup> under individual routine culture conditions as previously described for laboratory A,<sup>8</sup> laboratory B,<sup>9</sup> and laboratory C.<sup>10</sup>

**Growth inhibition assays:** Antimalarial activities (presented as IC<sub>50</sub> values (Table 2) on the chloroquine sensitive 3D7 strain and the CQ resistant Dd2 strain) of compounds **1c**, **3c**, **4c**, **7c**, **7i**, **7j**, and CQ were determined in laboratory C by the [<sup>3</sup>H] hypoxanthine incorporation assay,<sup>11</sup> as described.<sup>10</sup>

***In vitro* drug interaction studies:** *In vitro* interactions between the benzylMD **1c** and derivatives (P\_TM101, **4c**) or experimental molecules (DFO, ML276, EGCG, CB83) were investigated using the fractional inhibitory concentration (FIC) index described in the established fixed-ratio isobologram method,<sup>12</sup> in which a two-dimensional array of serial concentrations of test compounds is used to demonstrate that paired combinations of agents can exert inhibitory effects that are higher (synergy;  $\Sigma$  FIC<sub>50</sub> < 1.0) or lower (antagonism;  $\Sigma$  FIC<sub>50</sub> > 1.0) than the sum of their effects alone. First, to assess the method, a paired combination of two separate **1c** stock solutions used at different ratio was tested and revealed a clear additive effect ( $\Sigma$  FIC<sub>50</sub> = 0.98 ± 0.02), as expected. These assays were performed in laboratory A (DFO, EGCG, P\_TM101, **4c**) or in laboratory B (ML276, CB83). Briefly, an asynchronous blood stage culture of *P. falciparum* strain 3D7 was incubated for 48 h in the presence of decreasing drug concentrations in a microtiter plate (1% parasitemia, 1.5-2 % haematocrit). Drugs were applied alone and in combination at fixed concentration ratios (ratio A : B (v:v) = 1:4, 2:3, (2.5:2.5), 3:2, 4:1) and analysed in threefold serial dilutions. IC<sub>50</sub> values of drugs A and B alone were determined on the same plate to ensure accurate calculation of drug interactions. Also, the lead parent benzylMD **1c** was combined to itself (control assay of additive) to estimate the impact of experimental errors introduced by handling. Parasite growth was assessed in laboratory A using a SYBRgreen protocol,<sup>8</sup> and in laboratory B by the [<sup>3</sup>H] hypoxanthine incorporation assay.<sup>9</sup> Arithmetical and graphical analyses of results were performed. For arithmetical analysis, the fractional inhibitory concentration (FIC) of each drug in a given combination was calculated according to the following definitions: FIC (A) = IC<sub>50</sub> of A in combination / IC<sub>50</sub> of A alone and FIC (B) = IC<sub>50</sub> of B in combination / IC<sub>50</sub> of B alone. The sum

<sup>6</sup> Müller, T. *et al.* Glutathione reductase-catalysed cascade of redox reactions to bioactivate potent antimalarial 1,4-naphthoquinones – a new strategy to combat malarial parasites. *J. Am. Chem. Soc.* **133**, 11557-11571 (2011).

<sup>7</sup> Trager, W. & Jensen, J. B. Human malaria parasites in continuous culture. *Science* **193**, 673–675 (1976).

<sup>8</sup> Ehrhardt, K. *et al.* The mitochondrial electron transport chain is dispensable for the antimalarial activities of methylene blue and the lead 1,4-naphthoquinone 2-[4-(trifluoromethyl)benzyl]-menadione. *Antimicrob. Agents Chemother.* **57**, 2114-2120 (2013).

<sup>9</sup> Fromentin Y. *et al.* Synthesis of novel guttiferone A derivatives: *in-vitro* evaluation toward *Plasmodium falciparum*, *Trypanosoma brucei* and *Leishmania donovani*. *Eur. J. Eur. Chem.* **65**, 284-294 (2013).

<sup>10</sup> Kasozi, D. *et al.* Real-time imaging of the intracellular glutathione redox potential in malaria parasite *Plasmodium falciparum*. *Plos Pathog.* **9**, e1003782 (2013).

<sup>11</sup> Desjardins, R. E. *et al.* Quantitative assessment of antimalarial activity *in vitro* by a semiautomated microdilution technique. *Antimicro. Agents Chemother.* **16**, 710-718 (1979).

<sup>12</sup> Fivelman, Q. L. *et al.* Modified fixed-ratio isobologram method for studying *in vitro* interactions between atovaquone and proguanil or dihydroartemisinin against drug-resistant strains of *Plasmodium falciparum*. *Antimicrob. Agents Chemother.* **48**, 4097-4102 (2004).

of FIC (A) and FIC (B) ( $\sum$  FIC) was established for each combination and then the mean value of the four  $\sum$  FICs was calculated. A mean  $\sum$  FIC = 1 was assumed to reflect an additive effect or indifferent interaction, a mean  $\sum$  FIC < 1 a synergistic interaction and a mean  $\sum$  FIC > 1 an antagonistic interaction between the tested drugs. The graphical presentation (isobolograms) was established by plotting pairs of FIC values of drug A and drug B for each combination.

The fixed-ratio isobologram method was not applicable for nicotinamide or 6-aminonicotinamide because it was not possible to determine their IC<sub>50</sub> values due to poor growth inhibition activities and poor solubility of the compounds. Though to explore the *in vitro* interactions, the IC<sub>50</sub> values of lead benzylMD **1c** were determined in the presence of a fixed dose of nicotinamide or 6-aminonicotinamide, which showed no inhibition of parasitic growth when applied alone. IC<sub>50</sub> values were determined in laboratory A using a SYBRgreen protocol.

***In vitro* interaction of the lead parent benzylMD 1c with the hGrx1-roGFP2 protein:** The recombinant hGrx1-roGFP2 protein was heterologously overexpressed and prepared for measurements as described.<sup>10</sup> In short, a stock solution of 5 mM **1c** in DMSO was diluted to 500  $\mu$ M, 50  $\mu$ M and 5  $\mu$ M in a standard reaction buffer (as described) and mixed with 1.25  $\mu$ M of purified and reduced hGrx1-roGFP2 protein to final concentrations of 1 mM, 100  $\mu$ M, 10  $\mu$ M, and 1  $\mu$ M in a 96-well plate. After 15 min, 4 h, and 24 h incubation at room temperature, the emission of hGrx1-roGFP2 (510 nm) was measured after excitation at 405 and 480 nm in a plate reader (M200, Tecan) with gains set to 75 and 60, respectively. We calculated the ratio of the emission (405/480 nm) and plotted it against time or concentration of antimalarial drugs. In addition, an excitation spectrum was scanned from 340-504 nm with emission at 530 nm after 15 min, 4 h, and 24 h incubation.

To exclude a direct interaction between **1c** and the redox probe, the inhibitor was first incubated with the isolated recombinant hGrx1-roGFP2 protein. After 5 min only the highest concentration of compound **1c** tested (1 mM corresponding to 20,000  $\times$  IC<sub>50</sub>, which is pharmacologically not relevant), led to a 405/488 nm ratio increase from 0.57 to 0.80 (1.4-fold change). In comparison, 1 mM of the oxidizing agent diamide (which served as positive control) led to a ratio increase from 0.57 to 3.8 (6.6-fold change) (Fig. S10a). This result was supported by spectral analyses (Fig. S10d). After 4 h and 24 h incubation with 1 mM **1c** the 405/488 nm ratios increased to 2.3 and 2.6, respectively, which was partially induced by the solvent DMSO at 24h (Figs. S10b and S10c), while lower concentrations showed hardly any effects. Again, these results were supported by spectral analyses (Figs. S10e and S10f). In summary, a direct interaction between compound **1c** and the redox sensor influencing the results at pharmacologically relevant concentrations could be excluded.

**Imaging of the glutathione redox state in *Plasmodium* after 1c treatment:** Cloning the glutathione redox sensor hGrx1-roGFP2 as well as cultivation, sorbitol synchronization, and transfection of the chloroquine-sensitive *P. falciparum* 3D7 strain were carried out in laboratory C as described.<sup>10</sup> *P. falciparum* 3D7<sup>hGrx1-roGFP2</sup>-parasitized RBCs were enriched and prepared for microscopy as described. Compound **1c** was freshly dissolved in DMSO [5 mM] and diluted in pre-warmed (37 °C) Ringer's solution. Immediately treatment 20 mM *N*-ethylmaleimide was added to the cells to non-reversibly block sulfhydryls. Microscopy was carried out as described.<sup>10</sup> In brief, we excited hGrx1-roGFP2 at 405 nm and at 488 nm and detected emissions at 500–530 nm. Images were analysed by a custom written MatLaB (The MathWorks, [www.mathwork.de](http://www.mathwork.de)) analysis suite (M.D. Fricker, Dept. Plant Sciences, Oxford). Images were corrected for autofluorescence bleeding into the 405 nm channel, the background for each channel was subtracted and the 405/488 nm ratio was computed on a pixel-by-pixel basis. The region of interest was a well-defined cytosolic area of morphologically intact parasites.

**Cultivation and separation of ring-parasitized RBC and control non-parasitized RBC, treated or not with the lead parent benzylMD 1c and phenylhydrazine:** *P. falciparum* parasites (Palo Alto strain, *Mycoplasma*-free) were cultivated in freshly drawn normal RBCs at 2% haematocrit and synchronized as described.<sup>13</sup> Briefly, schizont stage parasitized normal RBCs (parasitemia > 95%) were mixed for invasion with washed normal RBCs and kept in growth medium (RPMI 1640, containing 25 mM HEPES, 30 mM glucose, 2 mM glutamine, 0.02 mM adenine, 24 mM NaHCO<sub>3</sub>, 32 µg/l gentamicin, and 10% A<sup>+</sup> decompartmented human plasma). After 19 h incubation in a humidified CO<sub>2</sub>/air incubator, the ring-enriched fraction was separated on and collected from a discontinuous 40/80/90% Percoll gradient (Sigma) containing mannitol (6% wt/vol). After 19 h incubation rings were enriched to approx. > 70% by the above procedure. Parasitemia and parasite morphology were assessed by light microscopy after Diff-Quik<sup>®</sup> Fix staining (Medion Diagnostics GmbH, Düringen, Switzerland). Non-parasitized control RBCs were incubated and treated in a similar way without schizont inoculation at time 0. Ring-parasitized and non-parasitized RBCs, treated or not with the lead benzylMD 1c 500 nM (10-fold IC<sub>50</sub>), 2.5 µM (50-fold IC<sub>50</sub>) or 5.0 µM (100-fold IC<sub>50</sub>) or supplemented with 2.0 mM phenylhydrazine, were suspended at 30% haematocrit in HANKS solution with 5.5 mM glucose, pH 7.45, and incubated at 37.5 °C. After 4 h incubation, hypotonic ghosts were prepared from the ring-enriched fraction (approx. 70% parasitemia) and from the non-parasitized control RBCs.

**Quantification of membrane-bound haemichromes in ghosts prepared from non-parasitized and ring-parasitized RBCs, and from non-parasitized G6PD-deficient RBCs:** Haem bound to the cytoplasmic face of the membrane as insoluble haemichromes was analysed in the hypotonic ghosts<sup>14</sup> prepared under non-reducing conditions in the presence of Complete<sup>®</sup> protease inhibitor and Trolox ((±)-6-Hydroxy-2,5,7,8-tetramethylchromane-2-carboxylic acid, Sigma, 100 µM final) cocktail from the ring-enriched fraction (approx. 70% parasitemia) and from the non-parasitized control RBCs.<sup>15</sup> Every ghost preparation was divided into two aliquots. A first aliquot of 15 µL ghosts was solubilized for 3 h at 4 °C in 1 mL of 0.1 N NaOH containing 3 mM EDTA and 0.05% (vol/vol) Triton X100 to quantify the total haem content (haemoglobin + insoluble haemichromes). A second aliquot of 15 µL ghosts was solubilized for 1 h at room temperature in 1 mL of PBS containing 3 mM EDTA and 0.05% (vol/vol) Triton X100 and used to quantify haemoglobin. Haem from both ghost aliquots was quantified by measuring the haem-dependent, luminol-enhanced luminescence as described.<sup>16</sup> Each luminescence measurement (5 µL aliquots) was repeated 3-4 times. Inter-measurement variability never exceeded 2-3%. The haemichrome content was calculated from the difference between total haem and haemoglobin haem. Haemichrome haem was the major component of total haem in control rings (88% of total haem), while membrane-bound haemoglobin was a minor fraction of total haem. Additional experiments using the same method described before were performed with non-parasitized G6PD-deficient RBC (Mediterranean variant with < 1% of normal enzyme activity) characterized by high sensitivity towards oxidants like diamide and phenylhydrazine.

---

<sup>13</sup> Turrini, F. *et al.* Phagocytosis of *Plasmodium falciparum*-infected human red blood cells by human monocytes: involvement of immune and nonimmune determinants and dependence on parasite developmental stage. *Blood* **80**, 801-808 (1992).

<sup>14</sup> Steck, T. *et al.* Inside-out red cell membrane vesicles: preparation and purification. *Science* **168**, 255-257 (1970).

<sup>15</sup> Ayi, K. *et al.* Enhanced phagocytosis of ring-parasitized mutant erythrocytes: a common mechanism that may explain protection against falciparum malaria in sickle trait and beta-thalassemia trait. *Blood* **104**, 3364-3371 (2004).

<sup>16</sup> Schwarzer, E. *et al.* A luminescence method for the quantitative determination of phagocytosis of erythrocytes, of malaria-parasitized erythrocytes and of malarial pigment. *Br. J. Haematol.* **88**, 740-745 (1994).

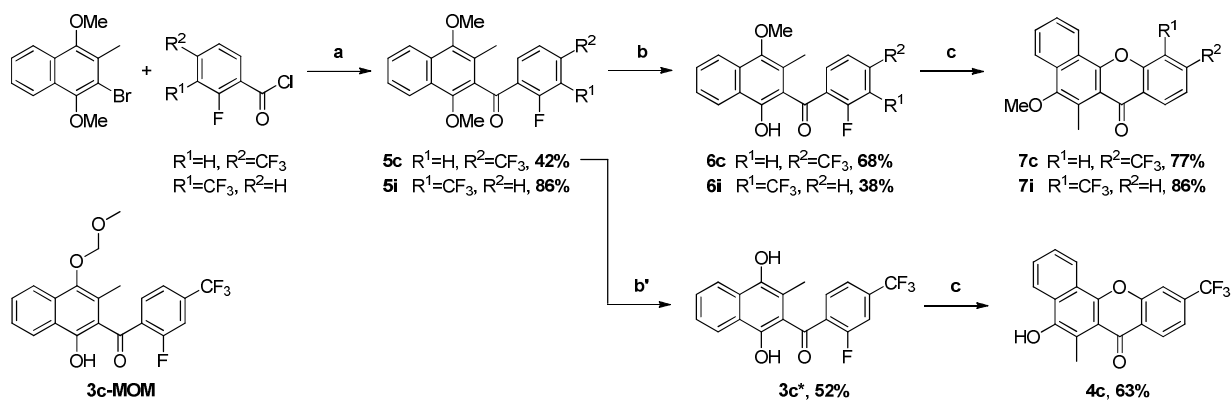


**Figure S1.** Three-step synthetic route to benzoxanthenes **4c** (LJ144, DAL105) and **7c**, **7i** and structure of the benzoylMD **3c-MOM**. Reagents and conditions: a) 1.0 equiv. bromonaphthalene, 1.1 equiv. 2-fluoro-benzoyl chloride, 1.1 equiv. BuLi, dry THF, -78 °C, 30 min; b) 1.0 equiv. BBr<sub>3</sub> (1 M in DCM), 0 °C, 2 h; c) 2.0 equiv. K<sub>2</sub>CO<sub>3</sub>, dry acetone, 50 °C, 2 h; b') 1.0 equiv. pure BBr<sub>3</sub>, 0 °C, 1 h. The preparation of the benzoyl-1-hydroxyMOM-protected-menadiol **3c-MOM** (DAL126) will be described elsewhere in a chemistry journal.

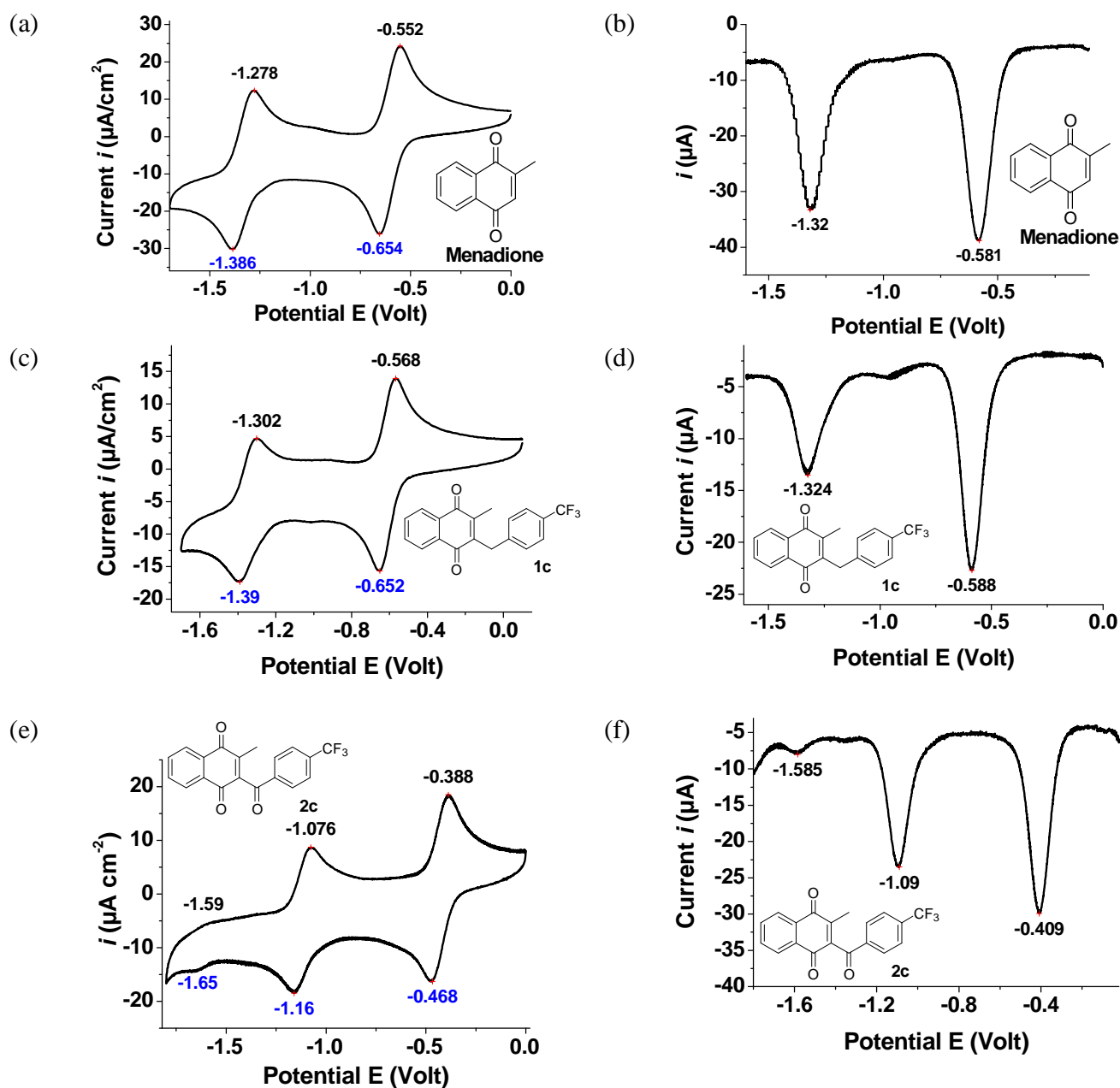


**Figure S2.** Cyclic voltammograms (a, c, e) and square wave differential pulse voltammograms (b, d, f) of menadione, benzylMD **1c**, benzoylMD **2c**, benzoxanthone **4c**, and the methoxylated benzoxanthone **7i** used as a model, recorded at 25.0 °C in argon-purged DMSO.

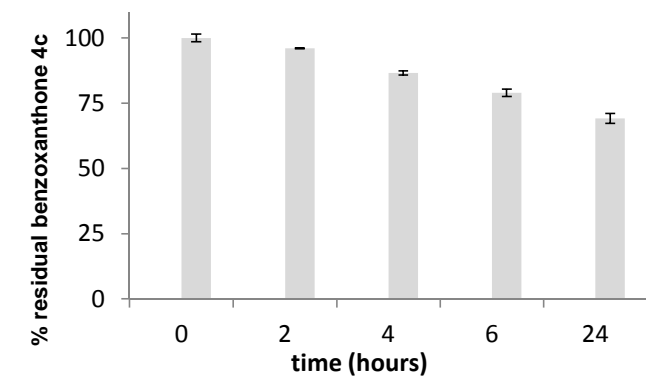
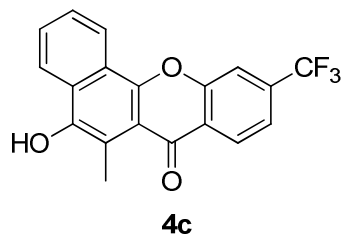
[menadione]<sub>0</sub> = 1.44 mM;  $I = 0.1 \text{ M NBu}_4\text{PF}_6$ ;  $\nu = 200 \text{ mV s}^{-1}$ . Reference Ag/AgCl.

[**1c**]<sub>0</sub> = 1.12 mM;  $I = 0.1 \text{ M NBu}_4\text{PF}_6$ ;  $\nu = 200 \text{ mV s}^{-1}$ .

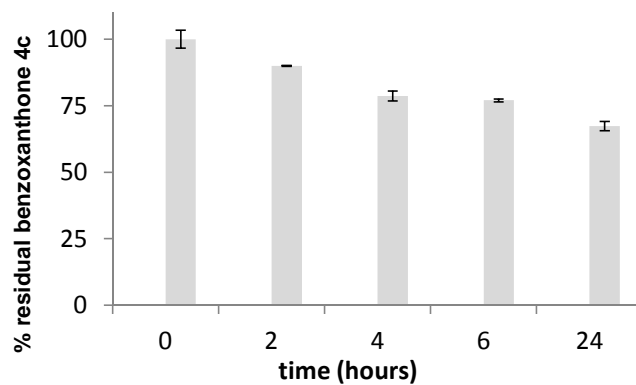
[**2c**]<sub>0</sub> = 1.30 mM;  $I = 0.1 \text{ M NBu}_4\text{PF}_6$ ;  $\nu = 200 \text{ mV s}^{-1}$ .

[**4c**]<sub>0</sub> = 1.17 mM;  $I = 0.1 \text{ M NBu}_4\text{PF}_6$ ;  $\nu = 200 \text{ mV s}^{-1}$ . The dashed line corresponds to CV of the background system (DMSO + 0.1 M NBu<sub>4</sub>PF<sub>6</sub>).

[**7i**]<sub>0</sub> = 1.21 mM;  $I = 0.1 \text{ M NBu}_4\text{PF}_6$ ;  $\nu = 200 \text{ mV s}^{-1}$ . The dashed line corresponds to CV of the background system (DMSO + 0.1 M NBu<sub>4</sub>PF<sub>6</sub>).



(a)

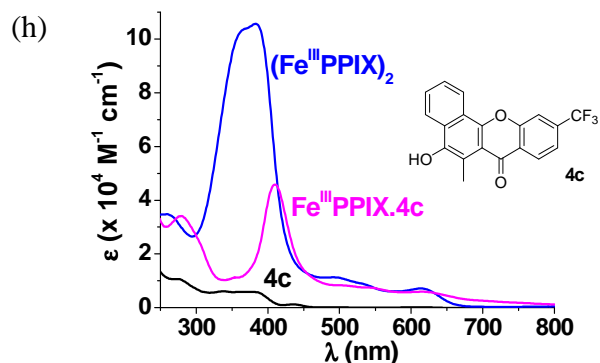
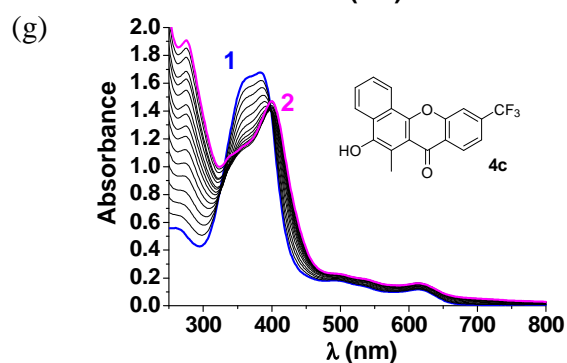
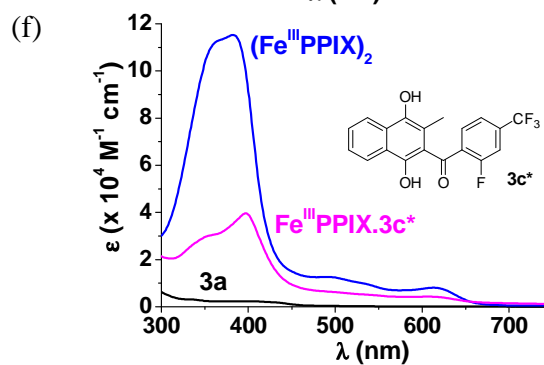
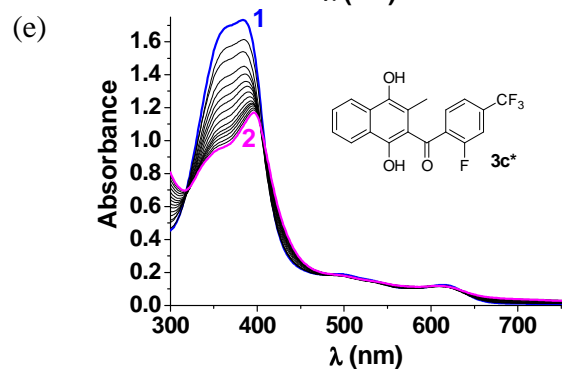
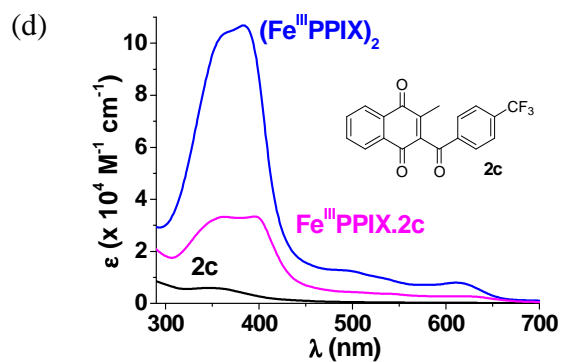
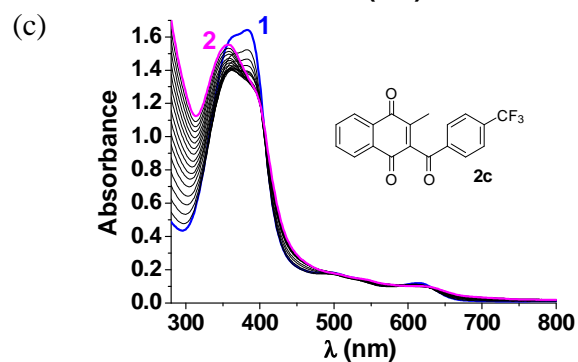
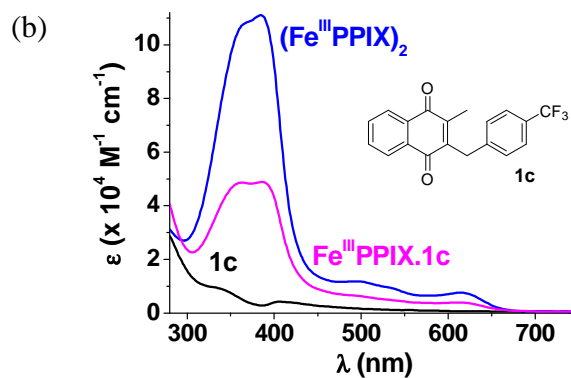
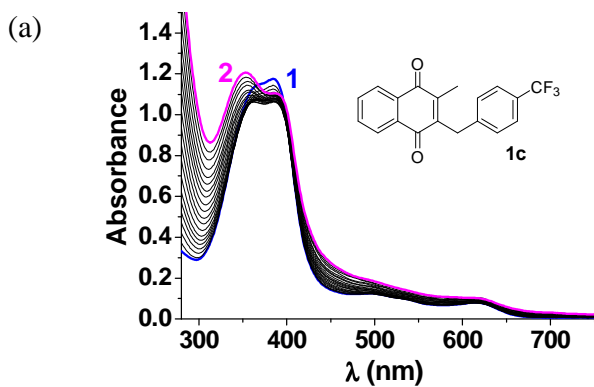


(b)

(a) pH 7.4	% <b>4c</b> at	t = 2 h	96.0	±	0.2
		t = 4 h	86.6	±	0.8
		t = 6 h	79.0	±	1.4
		t = 24 h	69.2	±	1.8
		$t_{1/2}$	> 24 h		

(b) pH 5.2	% <b>4c</b> at	t = 2 h	90.0	±	0.1
		t = 4 h	78.7	±	1.8
		t = 6 h	77.0	±	0.6
		t = 24 h	67.3	±	1.8
		$t_{1/2}$	> 24 h		

**Figure S3.** Stability of the benzoxanthone **4c** in aqueous buffer (a) at pH 7.4 (phosphate buffer) and (b) at pH 5.2 (acetate ammonium buffer) at 22 °C.





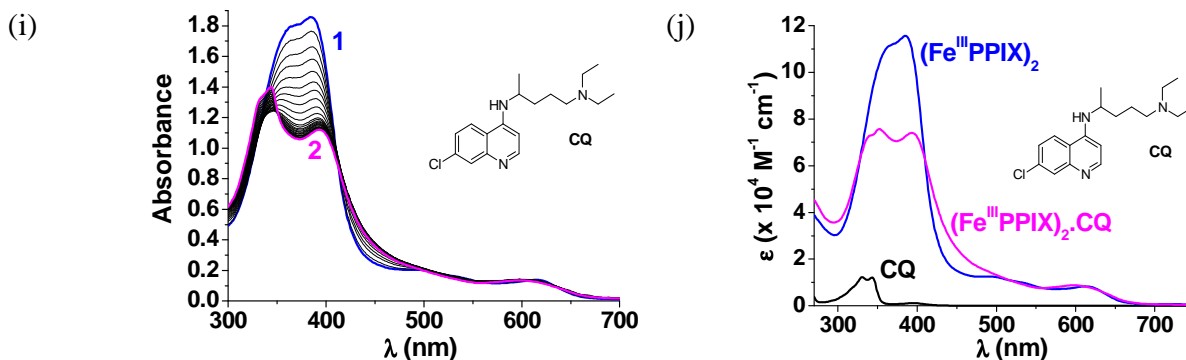


**Figure S4.** (left column) Spectrophotometric titration of haem (under its  $\pi$ - $\pi$  dimeric form,  $\log K_{\text{Dim}} = 6.82$ ) by benzylMD **1c**, benzoylMD **2c**, reduced benzoylMD **3c\***, benzoxanthone **4c**, and chloroquine (**CQ**), and (right column) electronic spectra of haem, of the free drugs, and of their corresponding  $\text{Fe}^{\text{III}}\text{PPIX}$ .drug complexes. Solvent: 0.2 M aqueous sodium HEPES buffer pH 7.5;  $T = 25.0 \text{ }^\circ\text{C}$ ;  $l = 1 \text{ cm}$ .

- (a)  $[\text{Fe}^{\text{III}}\text{PPIX}]_0 = 2.09 \times 10^{-5} \text{ M}$ ; (1)  $[\mathbf{1c}]_0/[\text{Fe}^{\text{III}}\text{PPIX}]_0 = 0$ ; (2)  $[\mathbf{1c}]_0/[\text{Fe}^{\text{III}}\text{PPIX}]_0 = 2.53$ .  
 (b)  $\log K_{\text{Fe}^{\text{III}}\text{PPIX} \cdot \mathbf{1c}} = 6.8 \pm 0.2$ .  
 (c)  $[\text{Fe}^{\text{III}}\text{PPIX}]_0 = 3.20 \times 10^{-5} \text{ M}$ ; (1)  $[\mathbf{2c}]_0/[\text{Fe}^{\text{III}}\text{PPIX}]_0 = 0$ ; (2)  $[\mathbf{2c}]_0/[\text{Fe}^{\text{III}}\text{PPIX}]_0 = 4.04$ .  
 (d)  $\log K_{\text{Fe}^{\text{III}}\text{PPIX} \cdot \mathbf{2c}} = 5.7 \pm 0.2$ .  
 (e)  $[\text{Fe}^{\text{III}}\text{PPIX}]_0 = 3.10 \times 10^{-5} \text{ M}$ ; (1)  $[\mathbf{3c*}]_0/[\text{Fe}^{\text{III}}\text{PPIX}]_0 = 0$ ; (2)  $[\mathbf{3c*}]_0/[\text{Fe}^{\text{III}}\text{PPIX}]_0 = 2.07$ .  
 (f)  $\log K_{\text{Fe}^{\text{III}}\text{PPIX} \cdot \mathbf{3c*}} = 6.1 \pm 0.1$ .  
 (g)  $[\text{Fe}^{\text{III}}\text{PPIX}]_0 = 3.0 \times 10^{-5} \text{ M}$ ; (1)  $[\mathbf{4c}]_0/[\text{Fe}^{\text{III}}\text{PPIX}]_0 = 0$ ; (2)  $[\mathbf{4c}]_0/[\text{Fe}^{\text{III}}\text{PPIX}]_0 = 4.2$ .  
 (h)  $\log K_{\text{Fe}^{\text{III}}\text{PPIX} \cdot \mathbf{4c}} = 5.5 \pm 0.2$ .  
 (i)  $[\text{Fe}^{\text{III}}\text{PPIX}]_0 = 3.36 \times 10^{-5} \text{ M}$ ; (1)  $[\text{CQ}]_0/[\text{Fe}^{\text{III}}\text{PPIX}]_0 = 0$ ; (2)  $[\text{CQ}]_0/[\text{Fe}^{\text{III}}\text{PPIX}]_0 = 1.03$ .  
 (j)  $\log \beta_{(\text{Fe}^{\text{III}}\text{PPIX})_2 \cdot \text{CQ}} = 13.17 \pm 0.07$ .

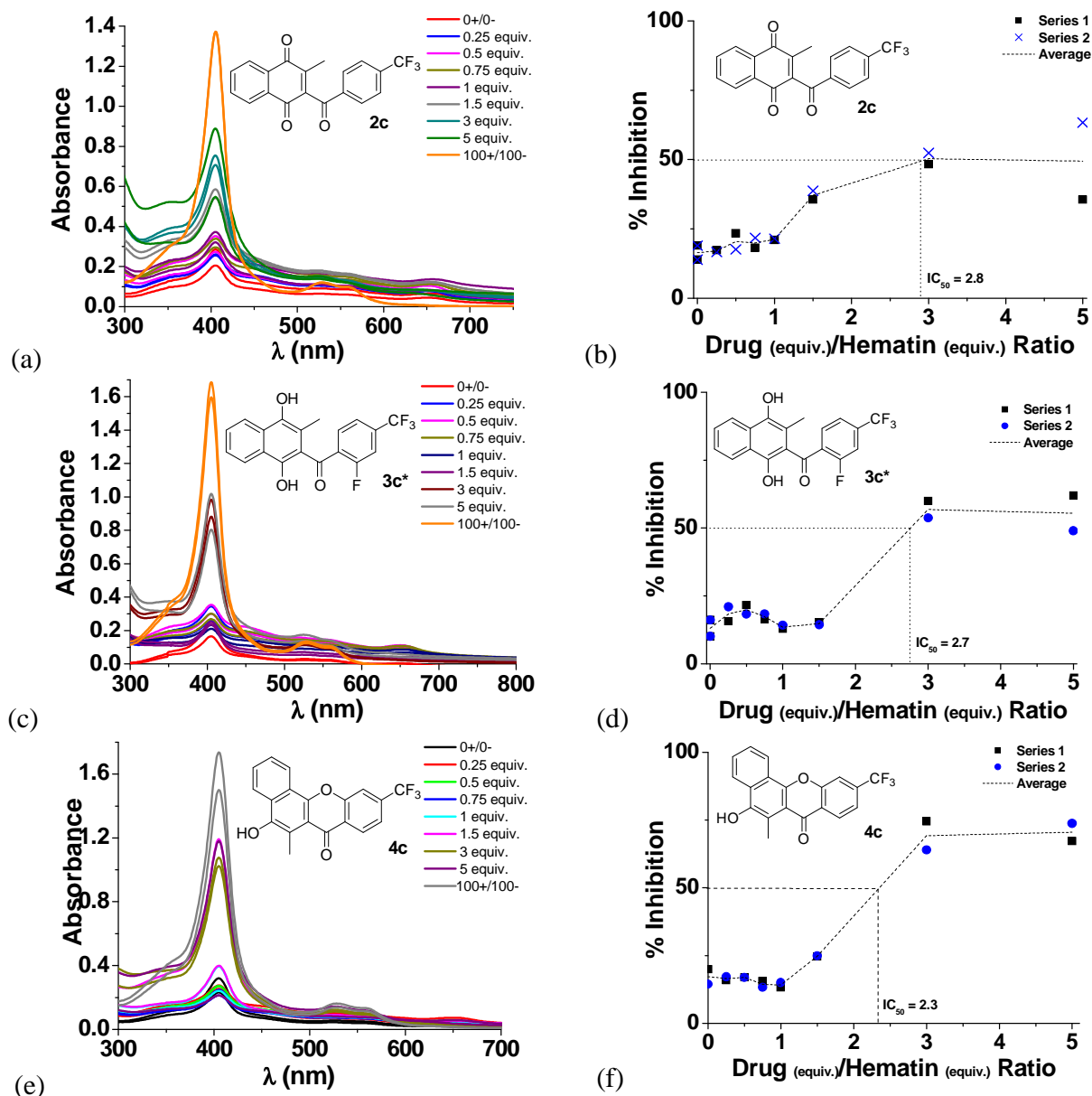
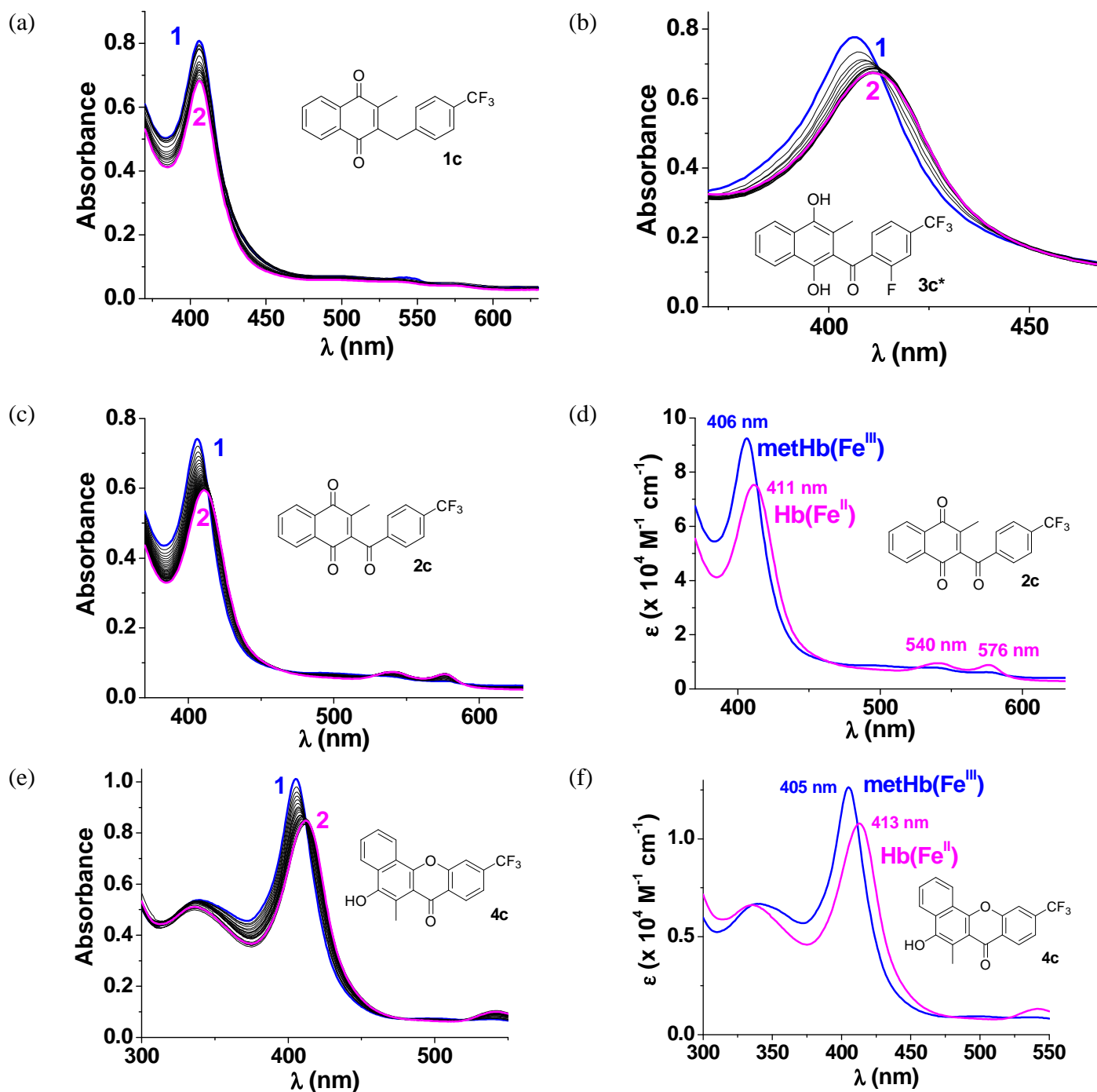


**Figure S5.** Inhibition of  $\beta$ -haematin crystallization by benzoylMD **2c**, reduced benzoylMD **3c\***, measured by UV-visible absorption spectrophotometry using pyridine (5% by volume) as reporting reagent. (a, c, e) UV-visible absorption spectra. (b, d, f) % of inhibition of  $\beta$ -haematin crystallization as a function of drug (equiv.) / haematin (equiv.) ratio. Solvent: 0.2 M + 0.02 M sodium HEPES buffer pH 7.5. The cross ( $\times$ ) and the square ( $\blacksquare$ ) labels correspond to two independent replicates, while the dash line corresponds to the averaged values.

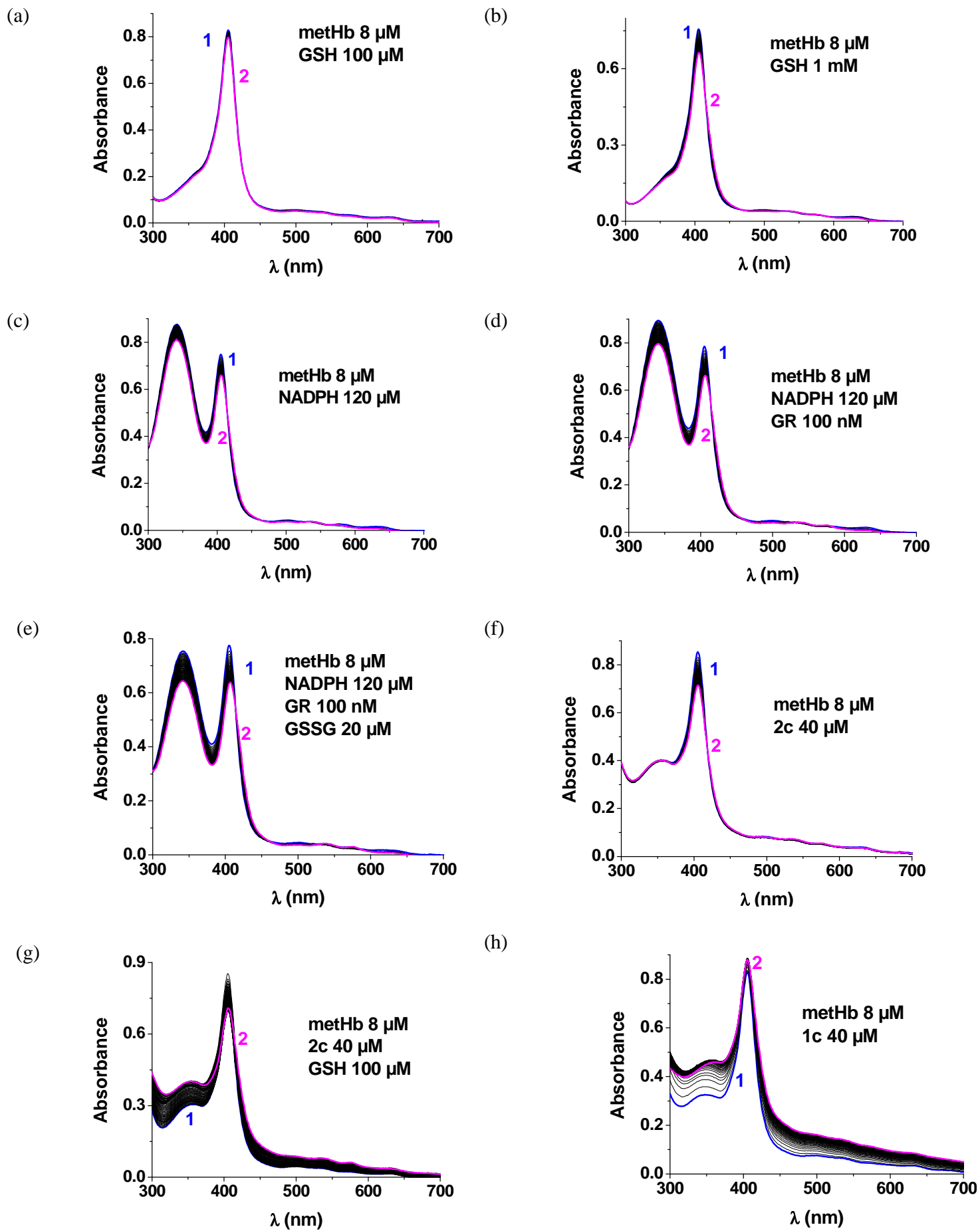
**2c:**  $IC_{50}$  (equivalent inhibitor) = 2.8; %<sub>max</sub> inhibition ~ 52%.

**3c\*:**  $IC_{50}$  (equivalent inhibitor) = 2.7; %<sub>max</sub> inhibition ~ 57%

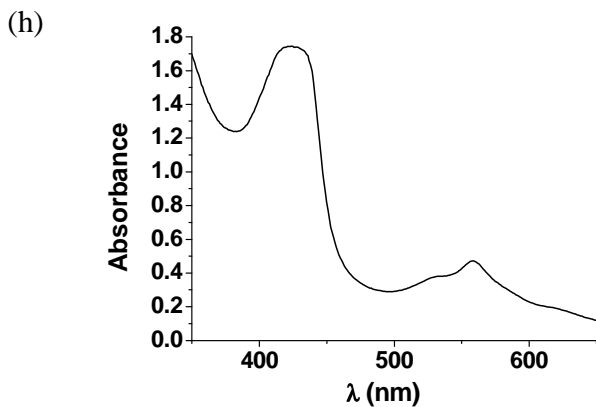
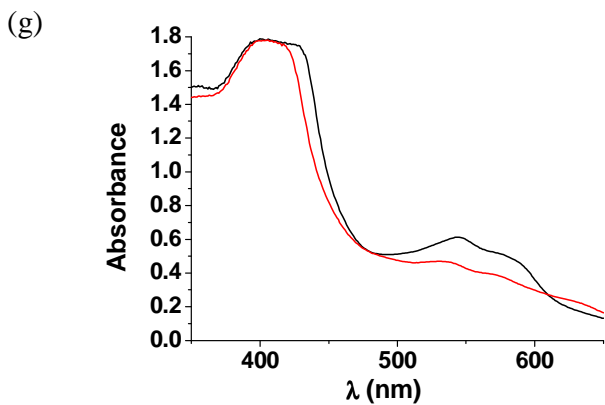
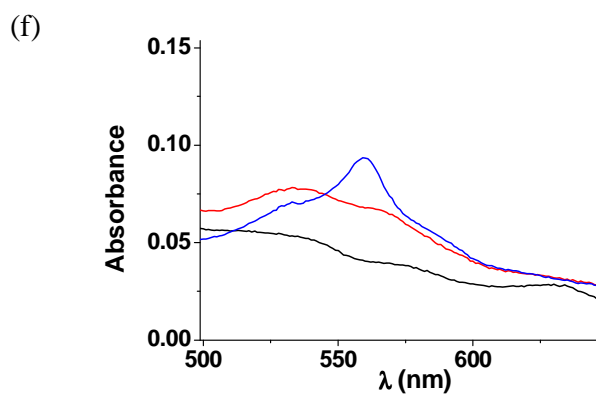
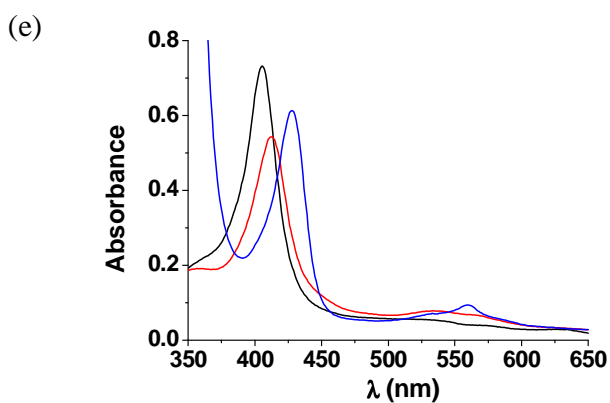
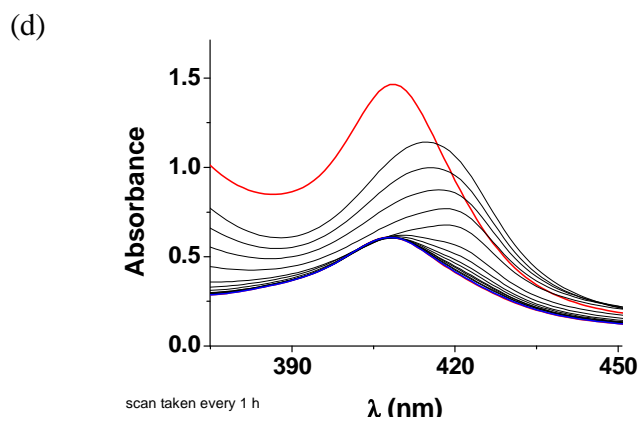
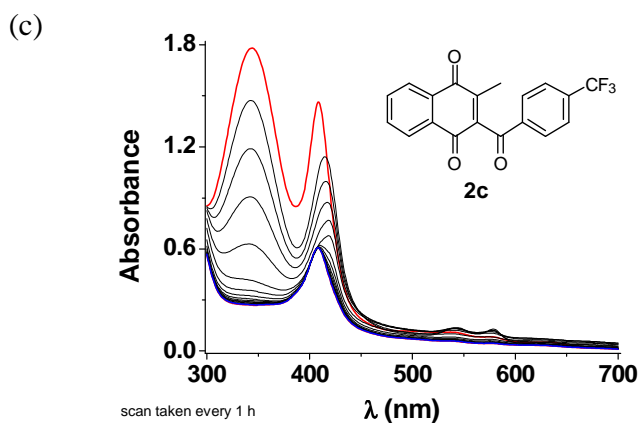
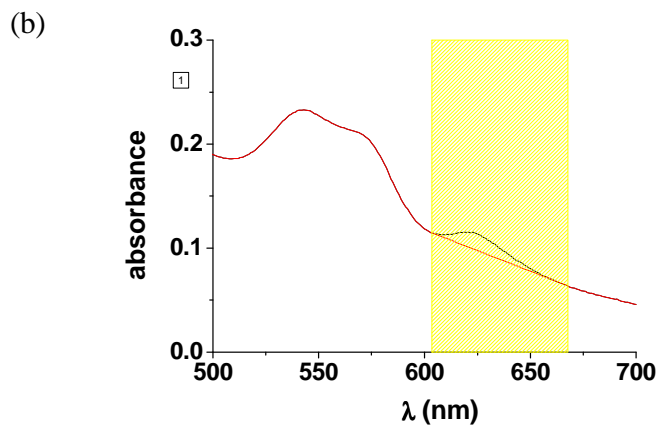
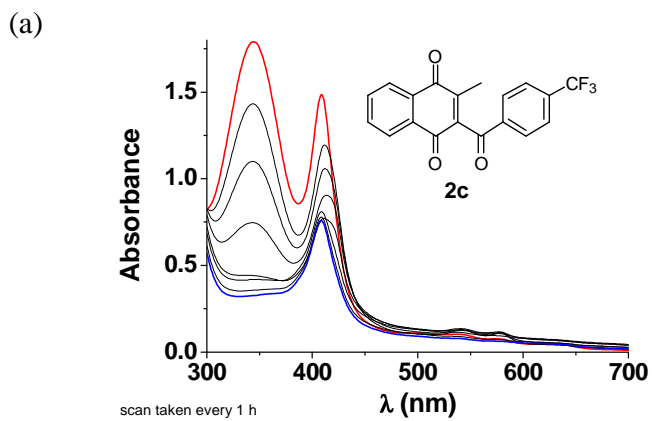
**4c:**  $IC_{50}$  (equivalent inhibitor) = 2.3; %<sub>max</sub> inhibition ~ 70%.



**Figure S6.** UV-visible absorption spectra recorded as a function of time in the coupled assay in the presence of the *hGR*/NADPH system. Plots showing (a) the absence of metHb(Fe<sup>III</sup>) reduction in the presence of benzylMD **1c** (121 μM NADPH + 81 nM *hGR* + 7.95 μM metHb + 40 μM **1c**) and (b) the direct metHb(Fe<sup>III</sup>) reduction in the presence of the reduced dihydrobenzoylMD **3c\*** (7.95 μM metHb + 50 μM **3c\***), respectively. Solvent: water (47 mM phosphate buffer pH 6.9 + 1 mM EDTA + 200 mM KCl); *T* = 25.0 °C; (1) *t* = 0; (2) *t* = 60 min. (c) Plot showing the metHb(Fe<sup>III</sup>) reduction in the presence of benzoylMD **2c** (no GSSG). (d) Electronic spectra of the reactants and the products of metHb(Fe<sup>III</sup>) reduction. Solvent: water (47 mM phosphate buffer pH 6.9 + 1 mM EDTA + 200 mM KCl); *T* = 25.0 °C; 121 μM NADPH + 81 nM *hGR* + 7.95 μM metHb + 40 μM **2c**; (1) *t* = 0; (2) *t* = 60 min. (e) Plot showing the metHb(Fe<sup>III</sup>) reduction in the presence of benzoxanthone **4c**. (f) Electronic spectra of the reactants and the products of metHb(Fe<sup>III</sup>) reduction. Solvent: water (47 mM phosphate buffer pH 6.9 + 1 mM EDTA + 200 mM KCl); *T* = 25.0 °C; 53 μM NADPH + 133 nM *hGR* + 7.95 μM metHb + 40 μM **4c**; (1) *t* = 0; (2) *t* = 19.8 min.



**Figure S7.** Controls showing the essential requirement of benzoylMD **2c** in the NADPH-dependent GR-mediated metHb reduction. Solvent: water (47 mM phosphate buffer pH 6.9 + 1 mM EDTA + 200 mM KCl); blue (1) t = 0 h, magenta (2) t = 2 h. (a) and (b) no influence of the reducing GSH at 100  $\mu$ M or 1 mM, respectively, on Hb generation; (c) no influence of NADPH on Hb generation; (d) No influence of NADPH/GR on Hb generation; (e) no influence of NADPH/GR/GSSG on Hb generation in the absence of the redox mediator; (f) no influence of **2c** on Hb generation in the absence of NADPH/GR; (g) GSH is not able to reduce **2c** to induce Hb generation; (h) no influence of benzylMD **1c** on metHb reduction in the absence of NADPH/GR.



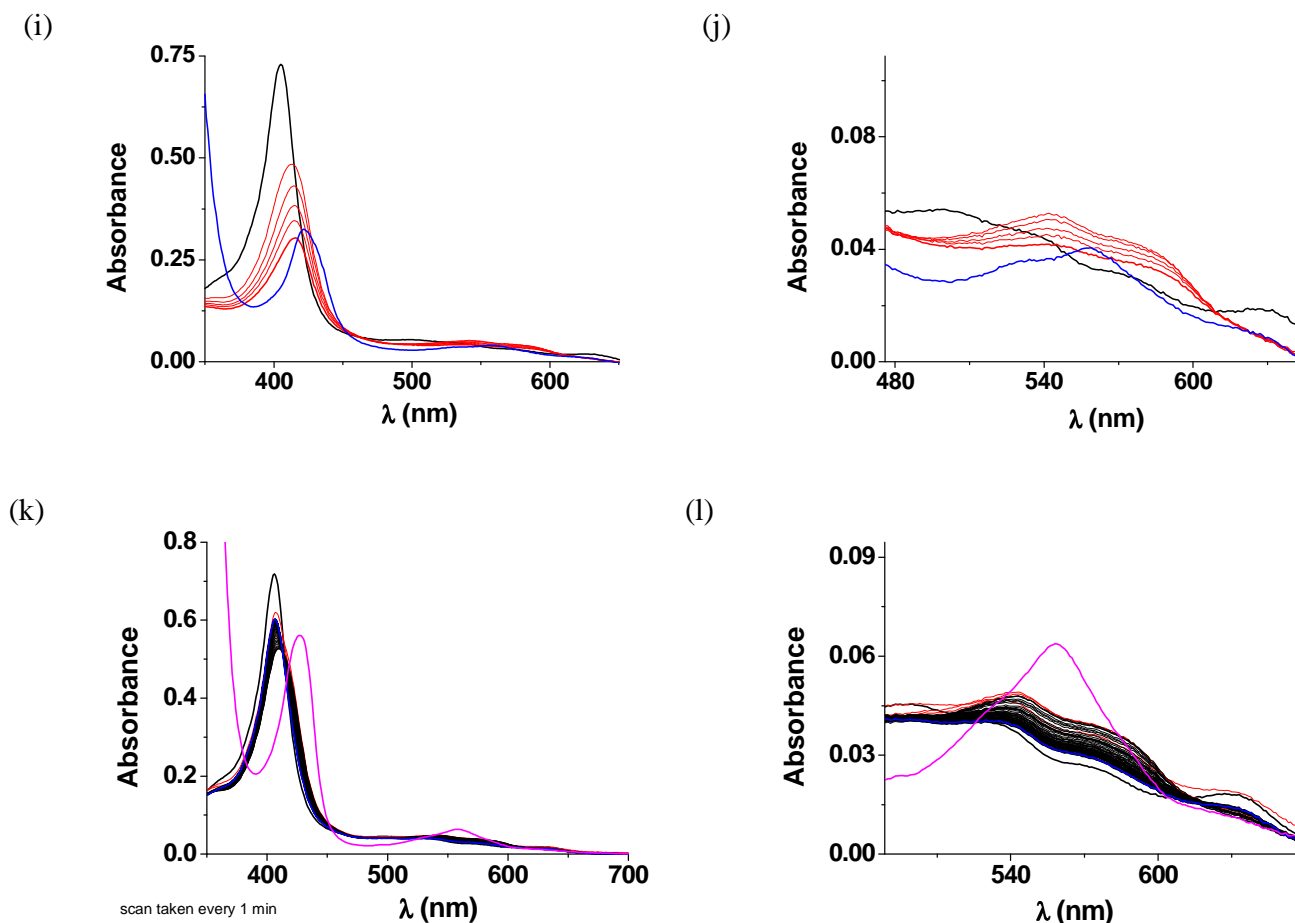
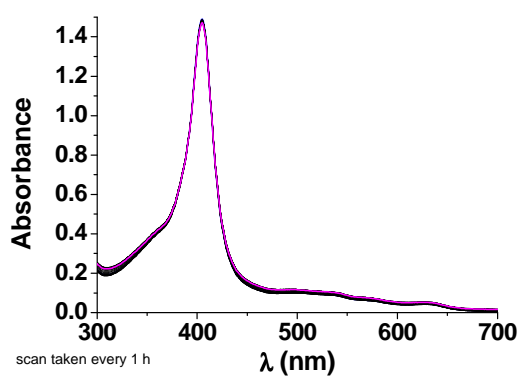
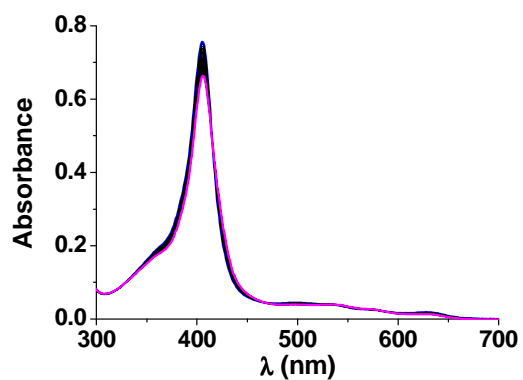


**Figure S8.** (a) UV-visible absorption spectra recorded as a function of time showing the metHb redox cycling in the presence of benzoylMD **2c**. Solvent: water (47 mM phosphate buffer pH 6.9 + 1 mM EDTA + 200 mM KCl). MetHb (32  $\mu$ M), benzoylMD **2c** (40  $\mu$ M), NADPH (480  $\mu$ M), SOD (7.2 U/mL) *PfGR* (400 nM), 25  $^{\circ}$ C; red curve=start (0 h), blue curve=end (7 h); (b) the indirect determination of ferrylHb: example after 1 h; the spectrum of sulfHb obtained after the addition of  $\text{Na}_2\text{S}$  with the integration of peak at 620 nm; (c) Solvent: water (47 mM phosphate buffer pH 6.9 + 1 mM EDTA + 200 mM KCl). MetHb (32  $\mu$ M), benzoylMD **2c** (40  $\mu$ M), NADPH (480  $\mu$ M), *PfGR* (400 nM), 25  $^{\circ}$ C; red curve=start (0 h), blue curve=end (7 h); (d) close-up of Soret band of spectra in figure c; (e) haemichrome and haemochrome reference spectra: fully-recorded spectrum, black curve: metHb (8  $\mu$ M) in phosphate buffer (pH 7), red curve: addition of SDS (16:1) to metHb  $\rightarrow$  irreversible haemichrome, blue curve: addition of  $\text{Na}_2\text{S}_2\text{O}_4$  to haemichrome  $\rightarrow$  haemochrome. (f) close-up of Q-band region of spectra in figure E; (g) ferrylHb autoreduction over 15 h: oxidation reaction of metHb (80  $\mu$ M) by  $\text{H}_2\text{O}_2$  (800  $\mu$ M) in phosphate buffer (pH 7), black curve: ferrylHb (start = 0 h), red curve: ferrylHb decay (end = 15 h); (h) addition of  $\text{Na}_2\text{S}_2\text{O}_4$  to solution after 15 h  $\rightarrow$  haemochrome; (i) the formation of ferrylHb by  $\text{H}_2\text{O}_2$ , continuously generated by glucose oxidase, and autoreduction of ferrylHb over 3 h leading to haemichrome (prove by conversion to haemochrome): fully-recorded spectrum: oxidation reaction of metHb (8  $\mu$ M), glucose oxidase (0.6  $\mu$ g/mL)/D-glucose (0.8 mM) system in phosphate buffer (pH 7), black curve: metHb (start = 0 h), red curve: ferrylHb formation and decay (end = 3 h); blue curve: addition of  $\text{Na}_2\text{S}_2\text{O}_4$  to solution after 3 h  $\rightarrow$  haemochrome; (j) close-up of Q-band region of spectra in figure I; (K) the formation of ferrylHb by  $\text{H}_2\text{O}_2$  over 2 minutes, addition of catalase, 60 min of reaction, addition of  $\text{Na}_2\text{S}_2\text{O}_4$  leading mainly to deoxyHb; (k) fully-recorded spectrum: oxidation reaction of metHb (8  $\mu$ M) by  $\text{H}_2\text{O}_2$  (80  $\mu$ M) in phosphate buffer (pH 7), black curve: metHb (start = 0 h), red curve: ferrylHb formation (2 min), blue curve: end of autoreduction (62 min), pink curve: addition of  $\text{Na}_2\text{S}_2\text{O}_4$  to solution after 62 min  $\rightarrow$  mainly deoxyHb; (l) close-up of Q-band region of spectra in figure K.



(a)



(b)

**Figure S9.** MetHb stability in aqueous buffer. (a) metHb (32 μM) over 24 h; solvent: water (47 mM phosphate buffer pH 6.9 + 1 mM EDTA + 200 mM KCl); blue = 0 h, magenta = 24 h,  $l = 1$  cm; (b) metHb (8 μM) over 2 h; solvent: water (47 mM phosphate buffer pH 6.9 + 1 mM EDTA + 200 mM KCl); blue = 0h, magenta = 2 h,  $l = 0.2$  mm.



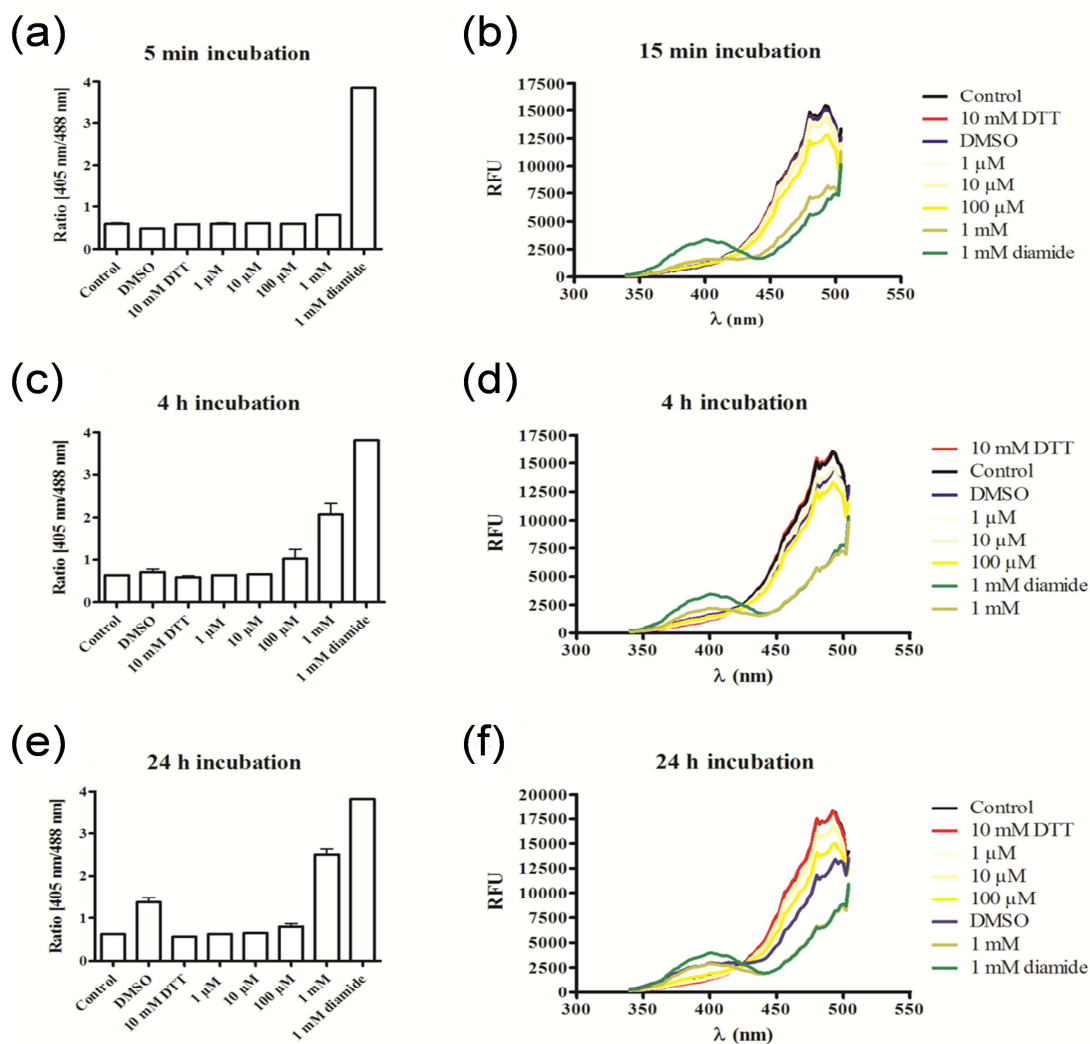
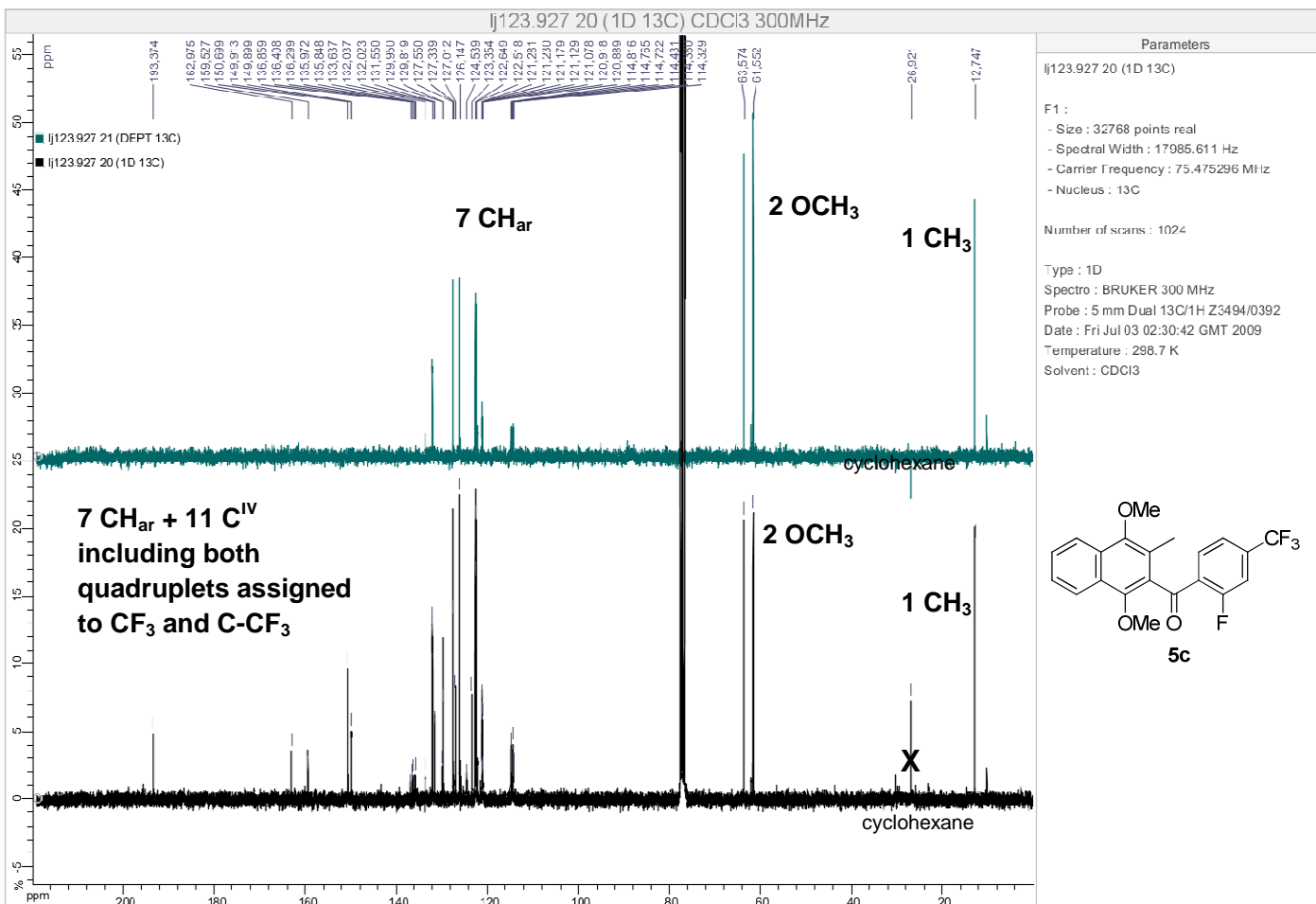
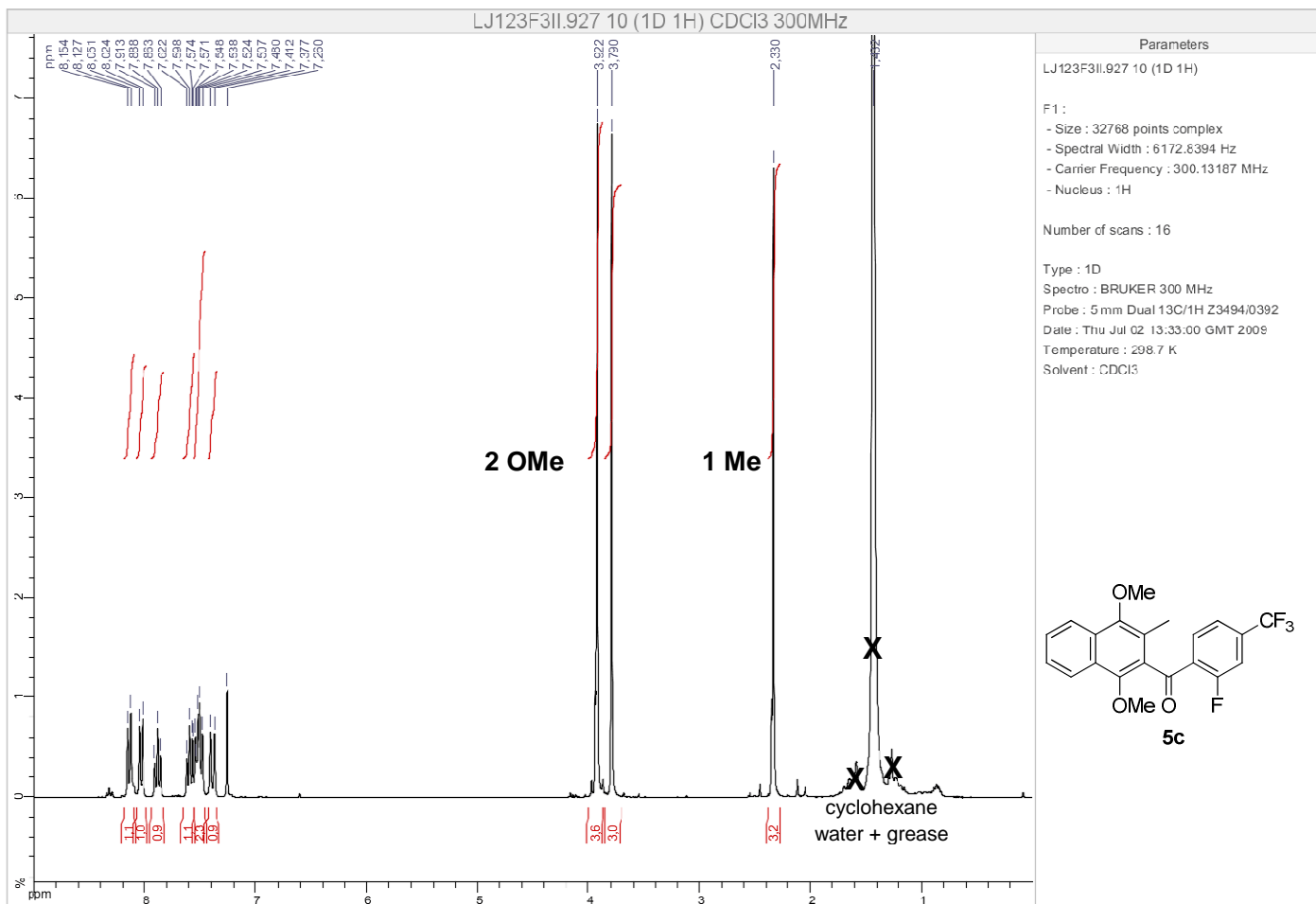
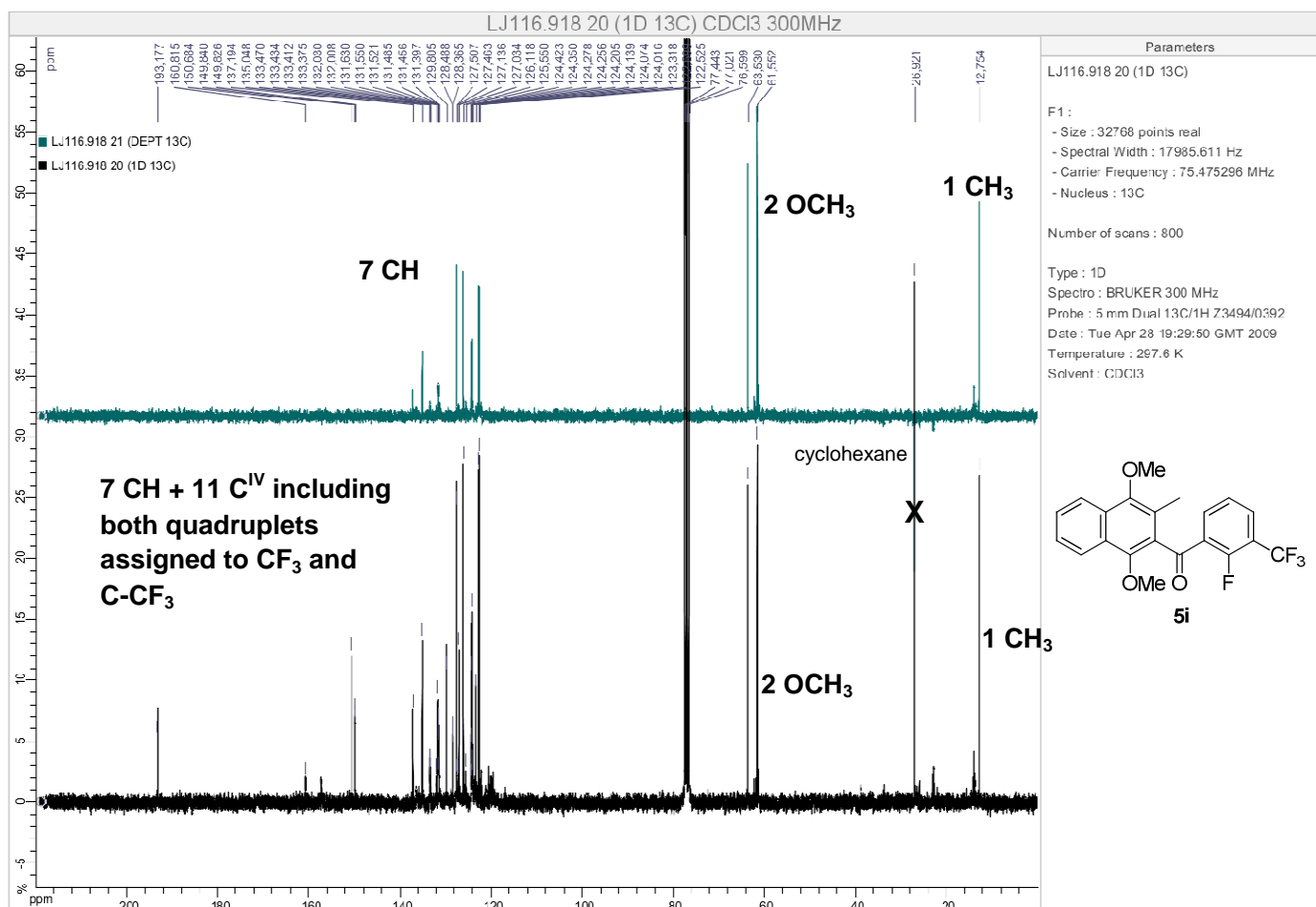
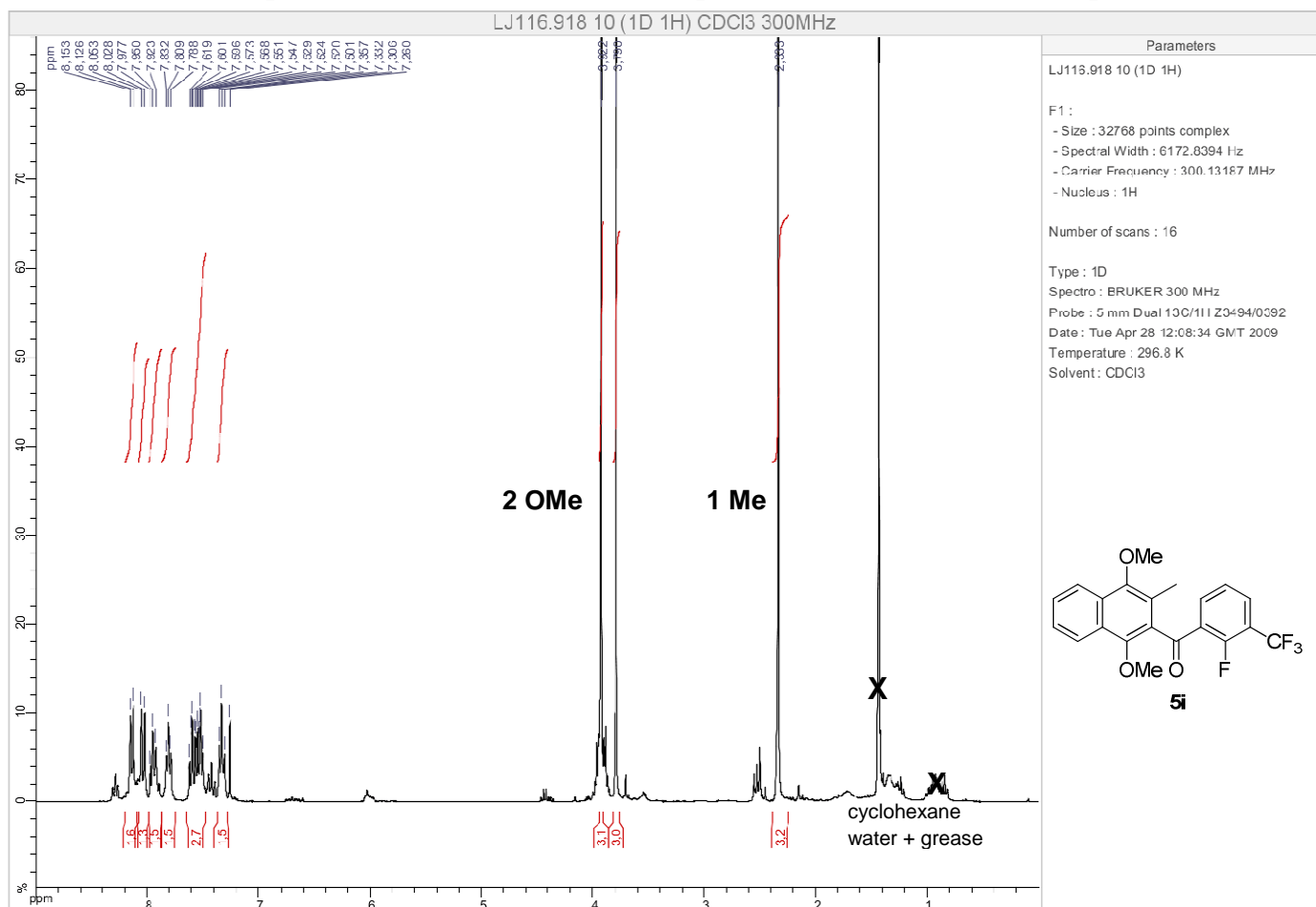


**Figure S10.** *In vitro* interaction of hGrx1-roGFP2 protein with the lead benzylMD **1c**. Compound **1c** at different concentrations was studied for its effects on the 405/480 nm ratio of isolated recombinant hGrx1-roGFP2 protein in a microplate reader (a) after 5 min, (b) after 4 h, and (c) after 24 h incubation. Each column represents mean values of three independent replicates. A spectral scan from 340 to 504 nm was carried out after (d) 15 min, (e) 4 h, and (f) 24 h incubation.

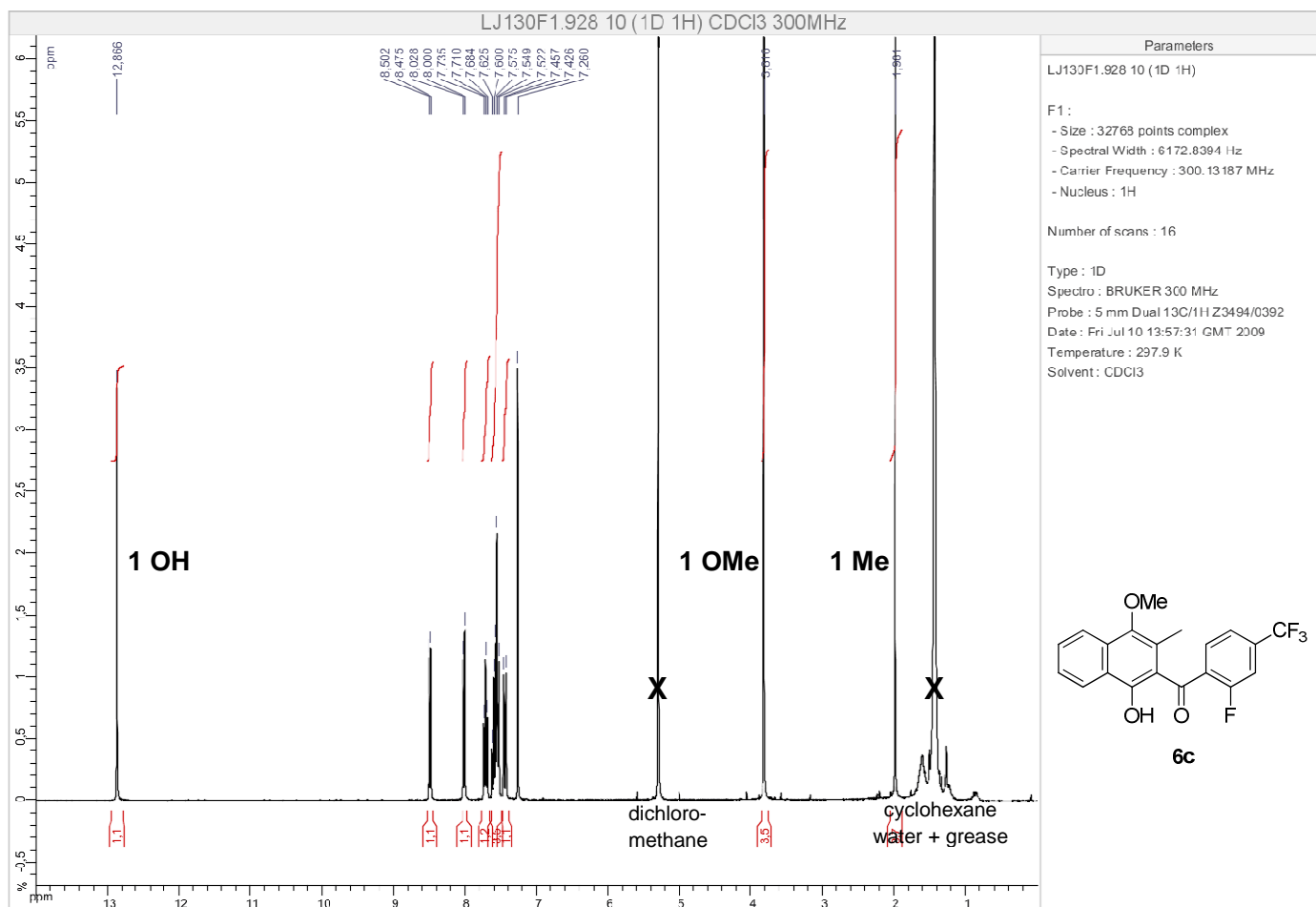
# NMR spectra of (1,4-dimethoxy-3-methylnaphthalen-2-yl)(2-fluoro-4-(trifluoromethyl)phenyl)methanone (5c): <sup>1</sup>H spectrum, <sup>13</sup>C & DEPT135 spectra.



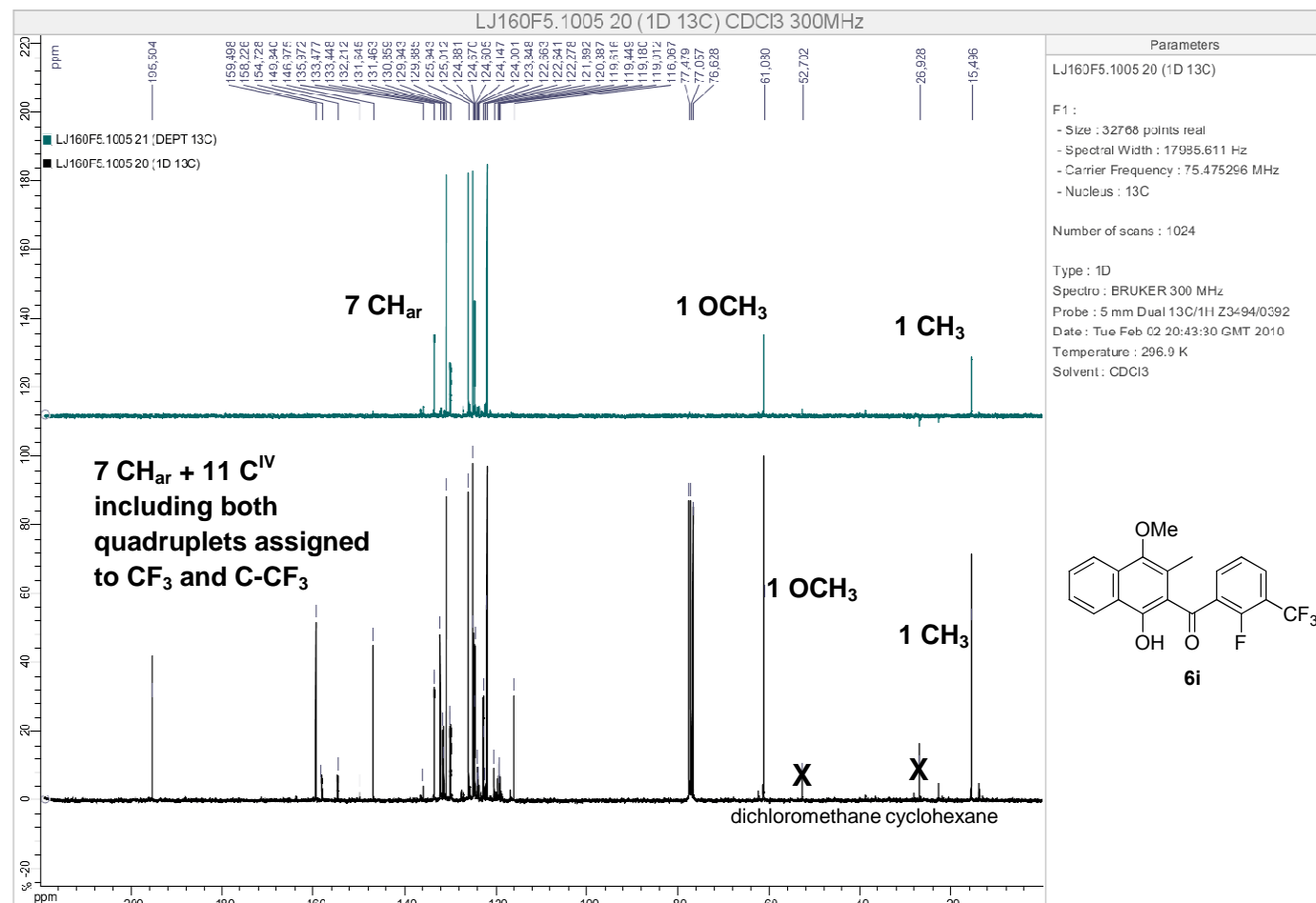
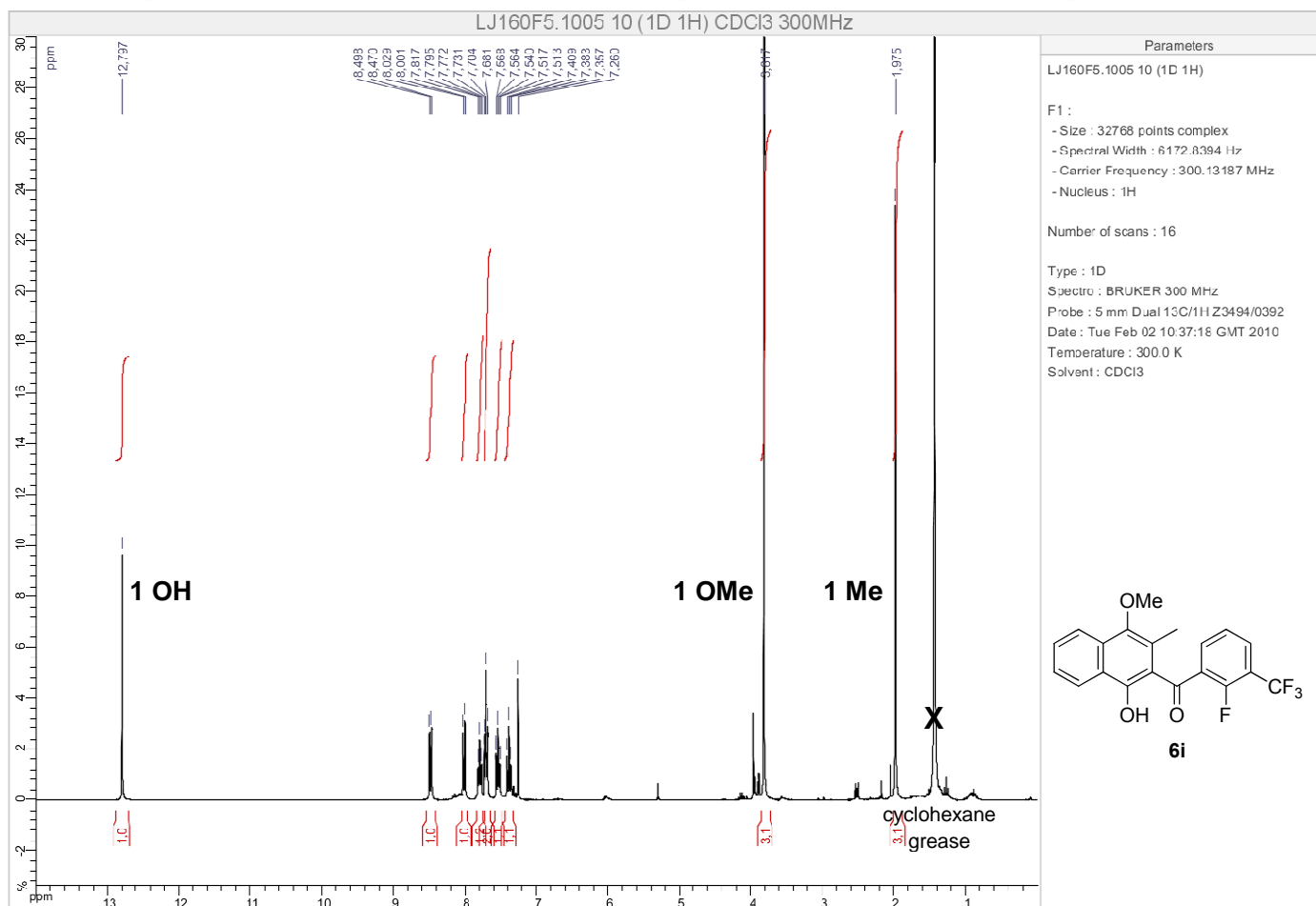
# NMR spectra of (1,4-dimethoxy-3-methylnaphthalen-2-yl)(2-fluoro-3-(trifluoromethyl)phenyl)methanone (**5i**): <sup>1</sup>H spectrum, <sup>13</sup>C & DEPT135 spectra.



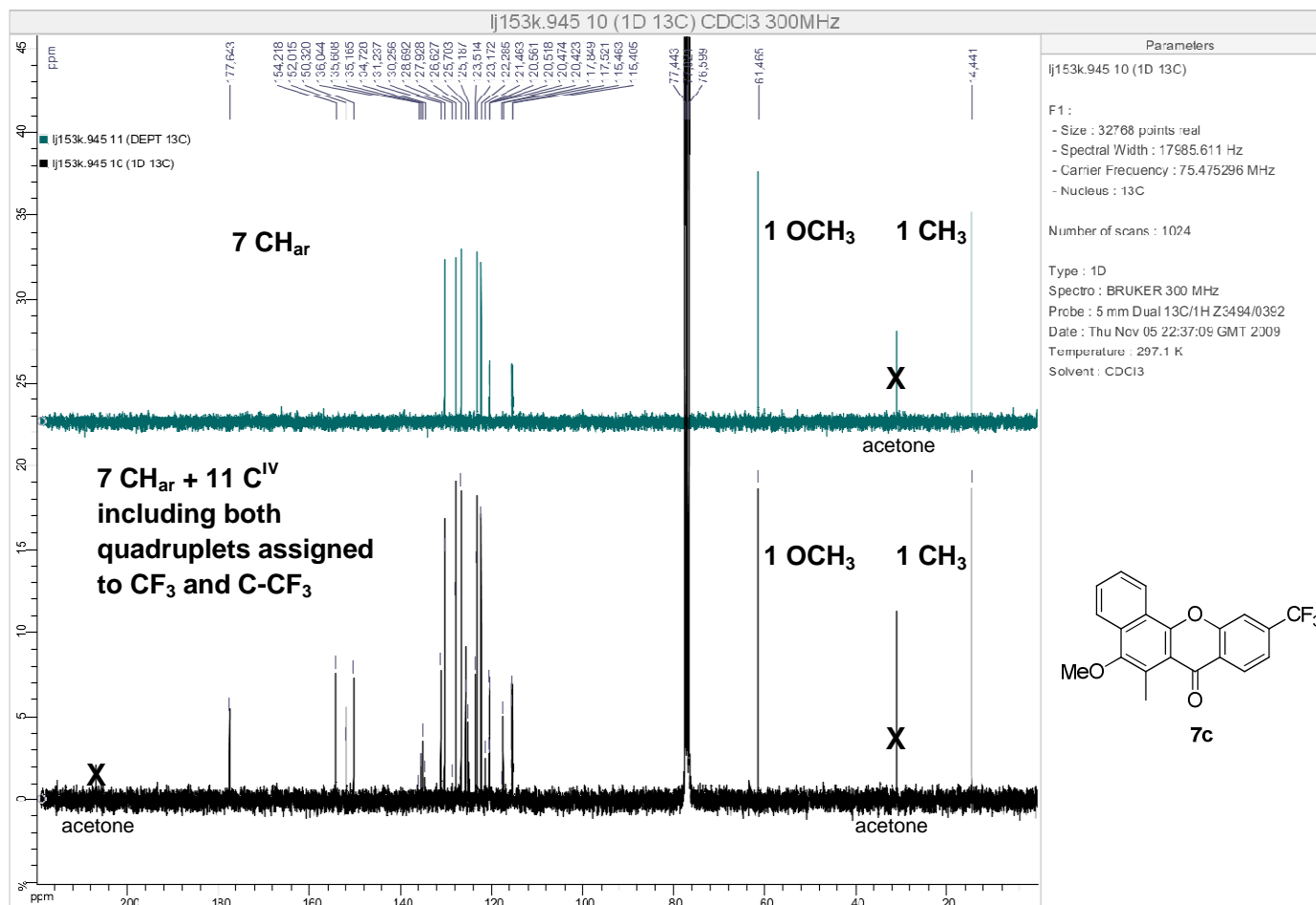
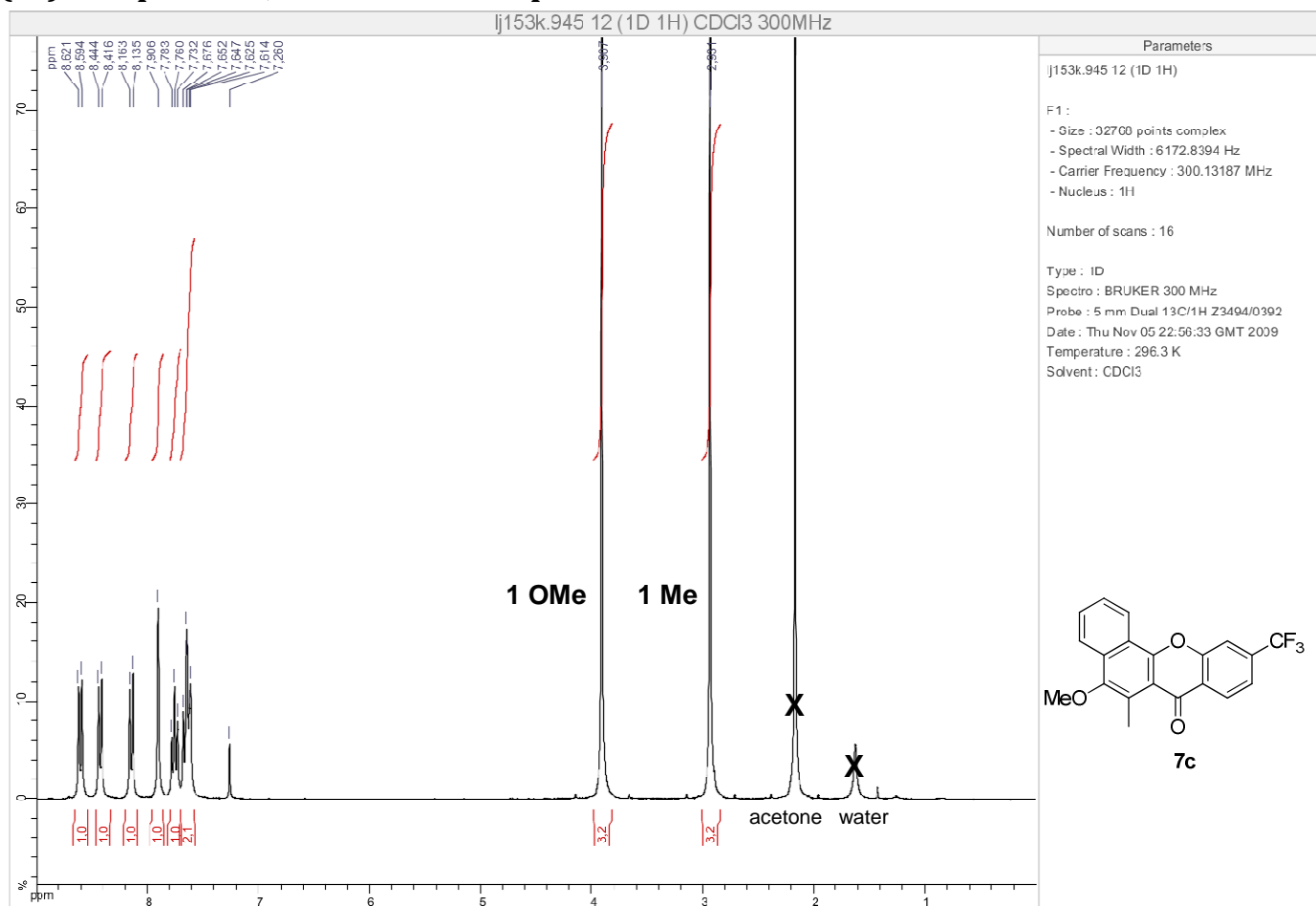
# <sup>1</sup>H NMR spectra of (2-fluoro-4-(trifluoromethyl)phenyl)(1-hydroxy-4-methoxy-3-methylnaphthalen-2-yl)methanone (6c).



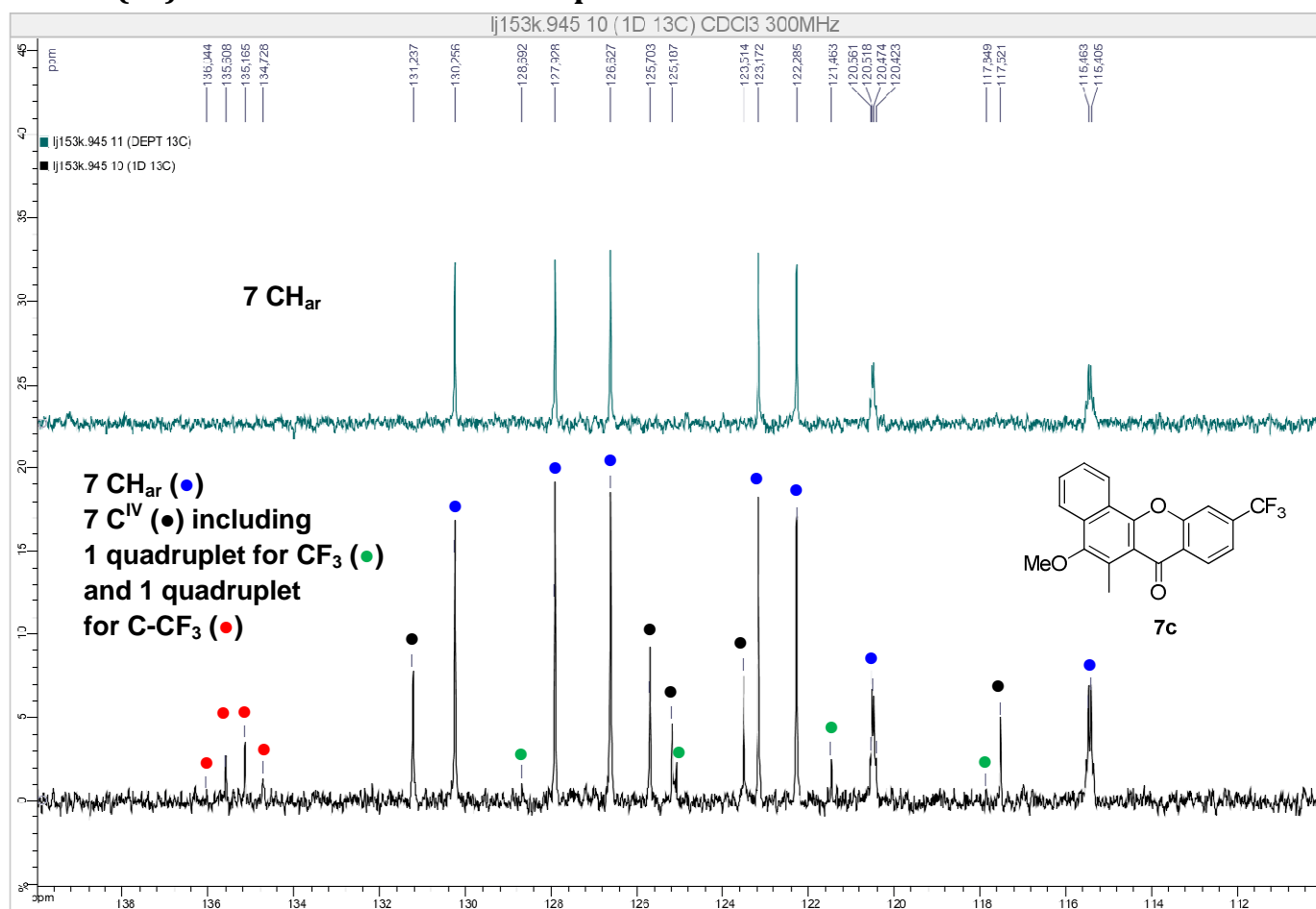
# NMR spectra of (2-fluoro-3-(trifluoromethyl)phenyl)(1-hydroxy-4-methoxy-3-methylnaphthalen-2-yl)methanone (6i): <sup>1</sup>H spectrum, <sup>13</sup>C & DEPT135 spectra.



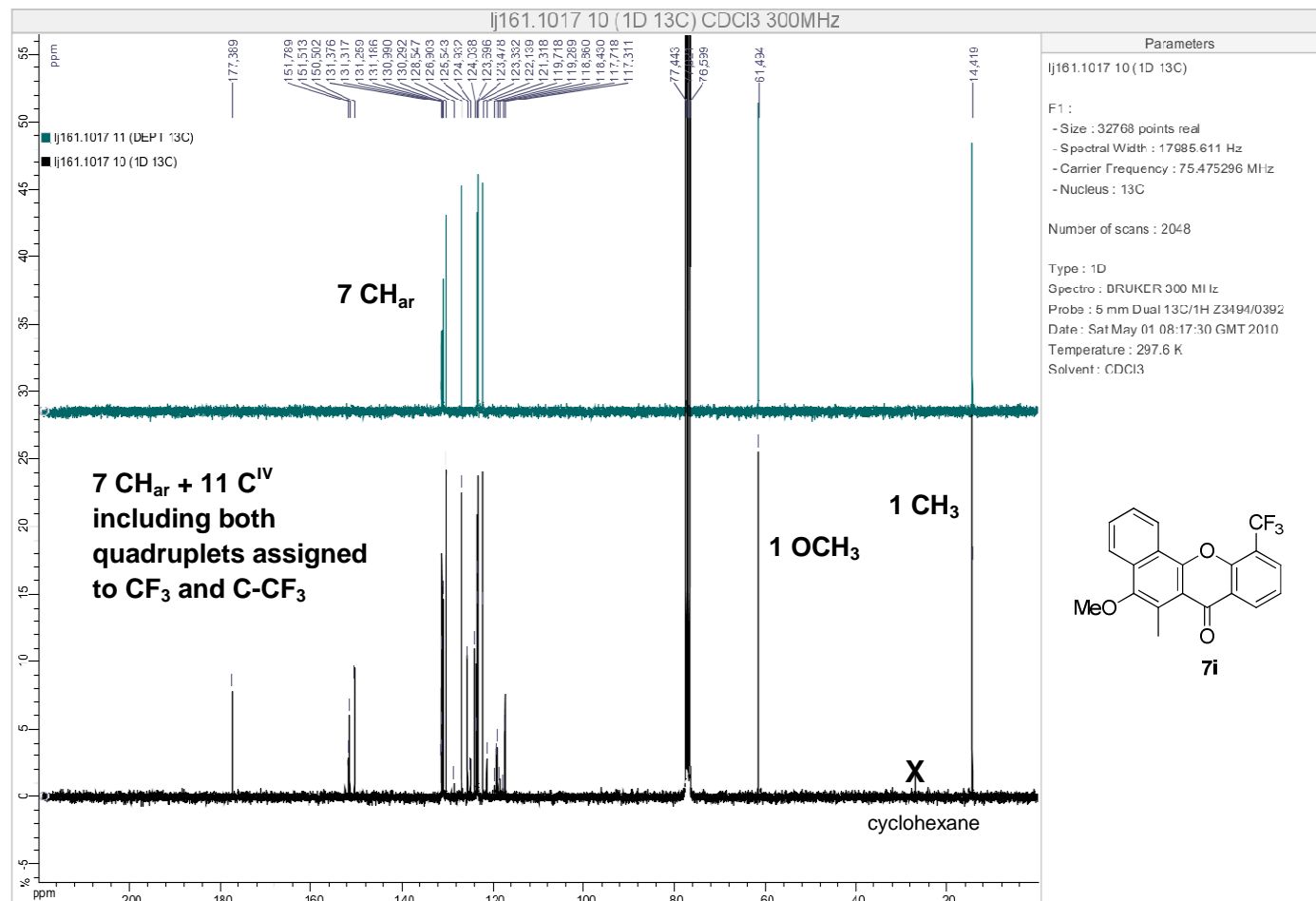
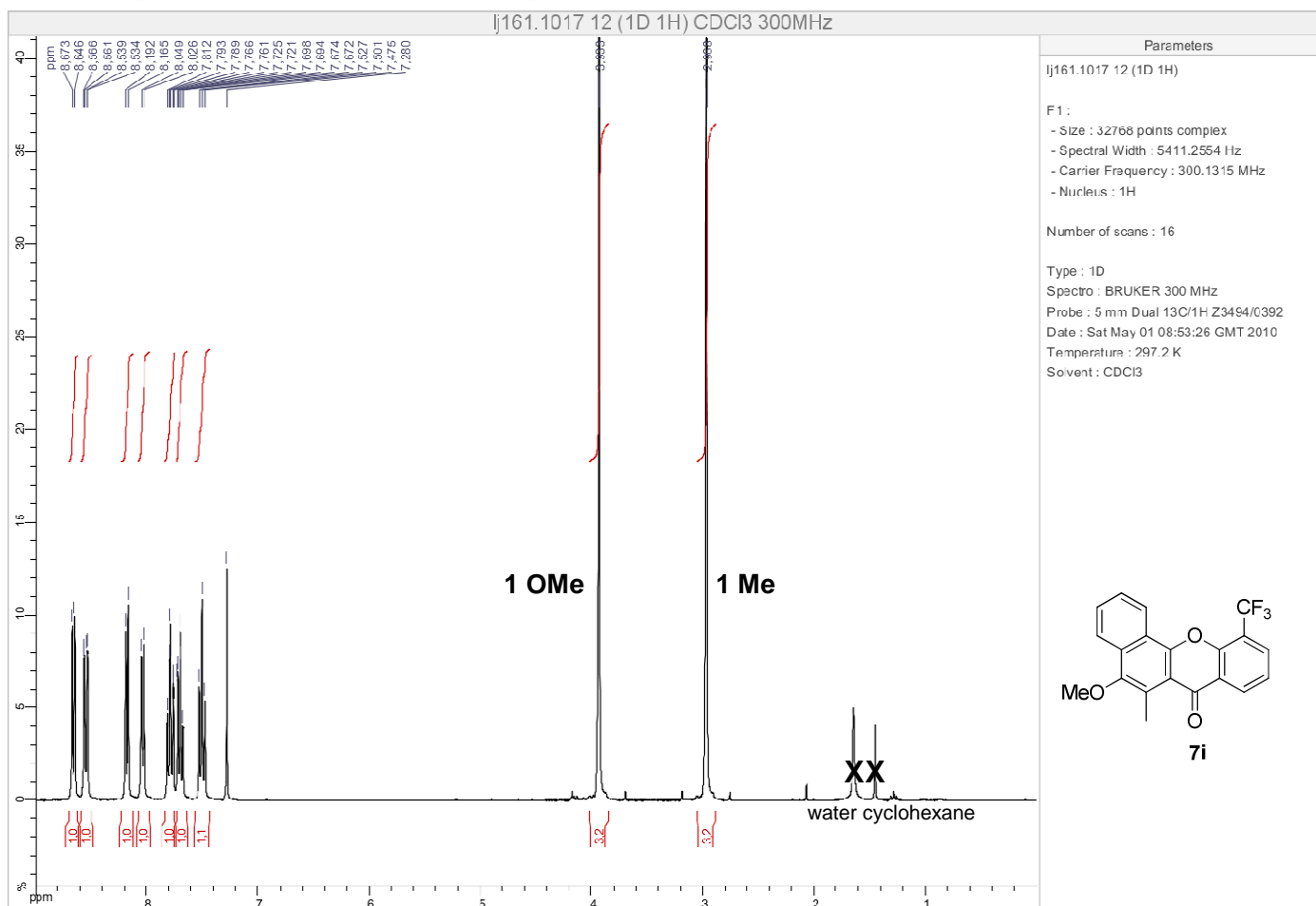
# NMR spectra of 5-methoxy-6-methyl-10-(trifluoromethyl)-7H-benzo[c]xanthen-7-one (7c): <sup>1</sup>H spectrum, <sup>13</sup>C & DEPT135 spectra.



# NMR spectra of 5-methoxy-6-methyl-10-(trifluoromethyl)-7H-benzo[c]xanthen-7-one (7c): zoom of <sup>13</sup>C & DEPT135 spectra.

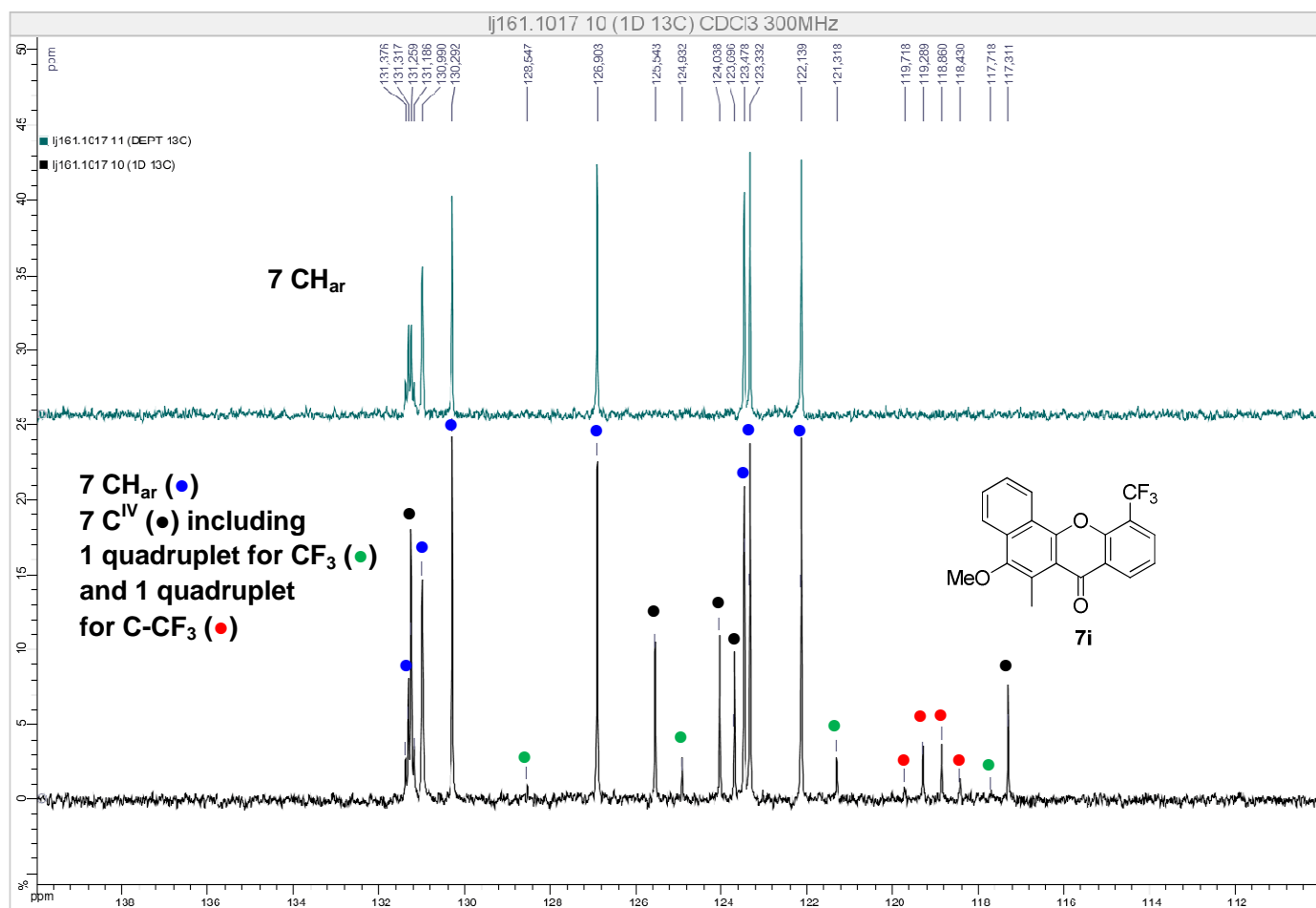


# NMR spectra of 5-methoxy-6-methyl-11-(trifluoromethyl)-7H-benzo[c]xanthen-7-one (7i): <sup>1</sup>H spectrum, <sup>13</sup>C & DEPT135 spectra.

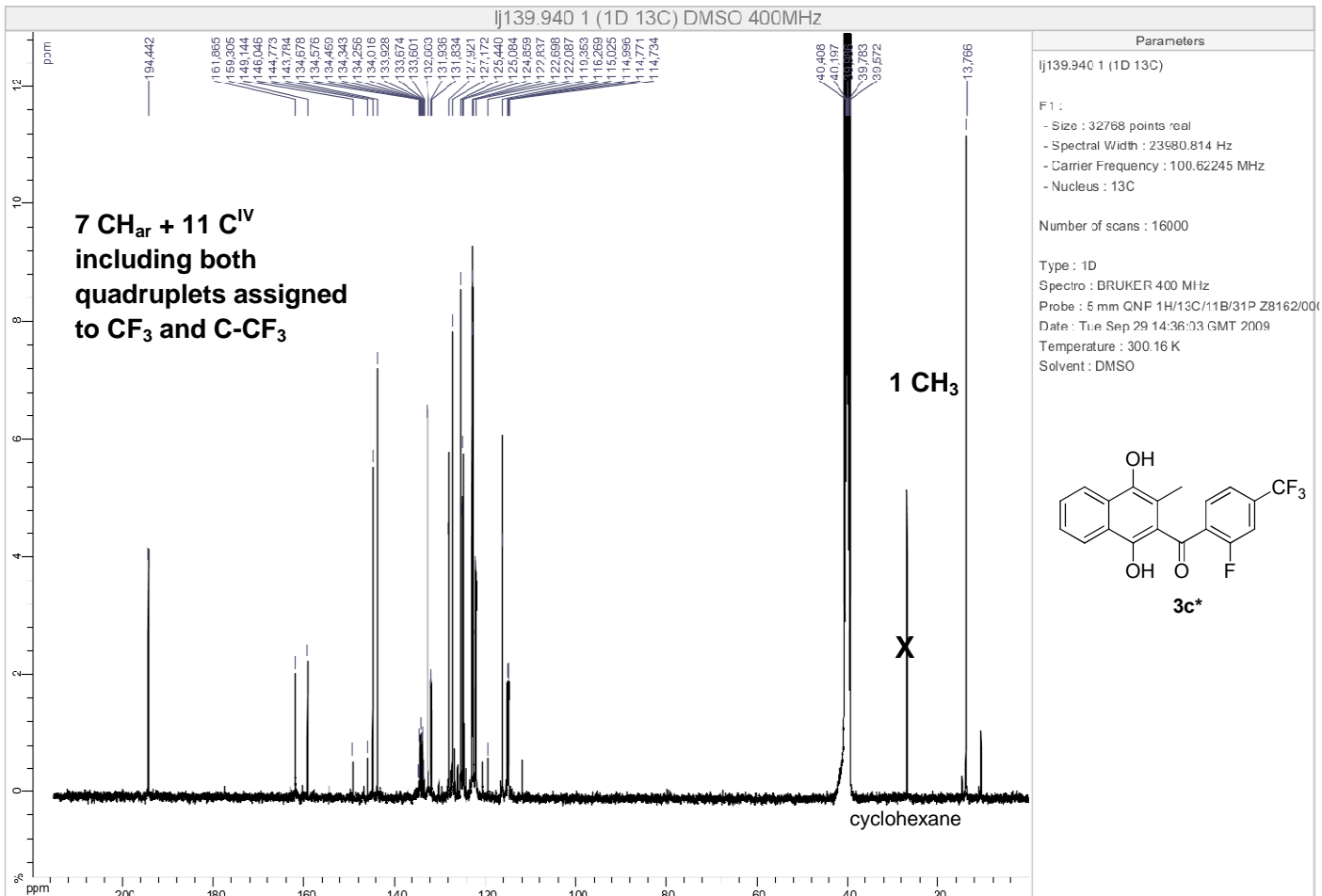
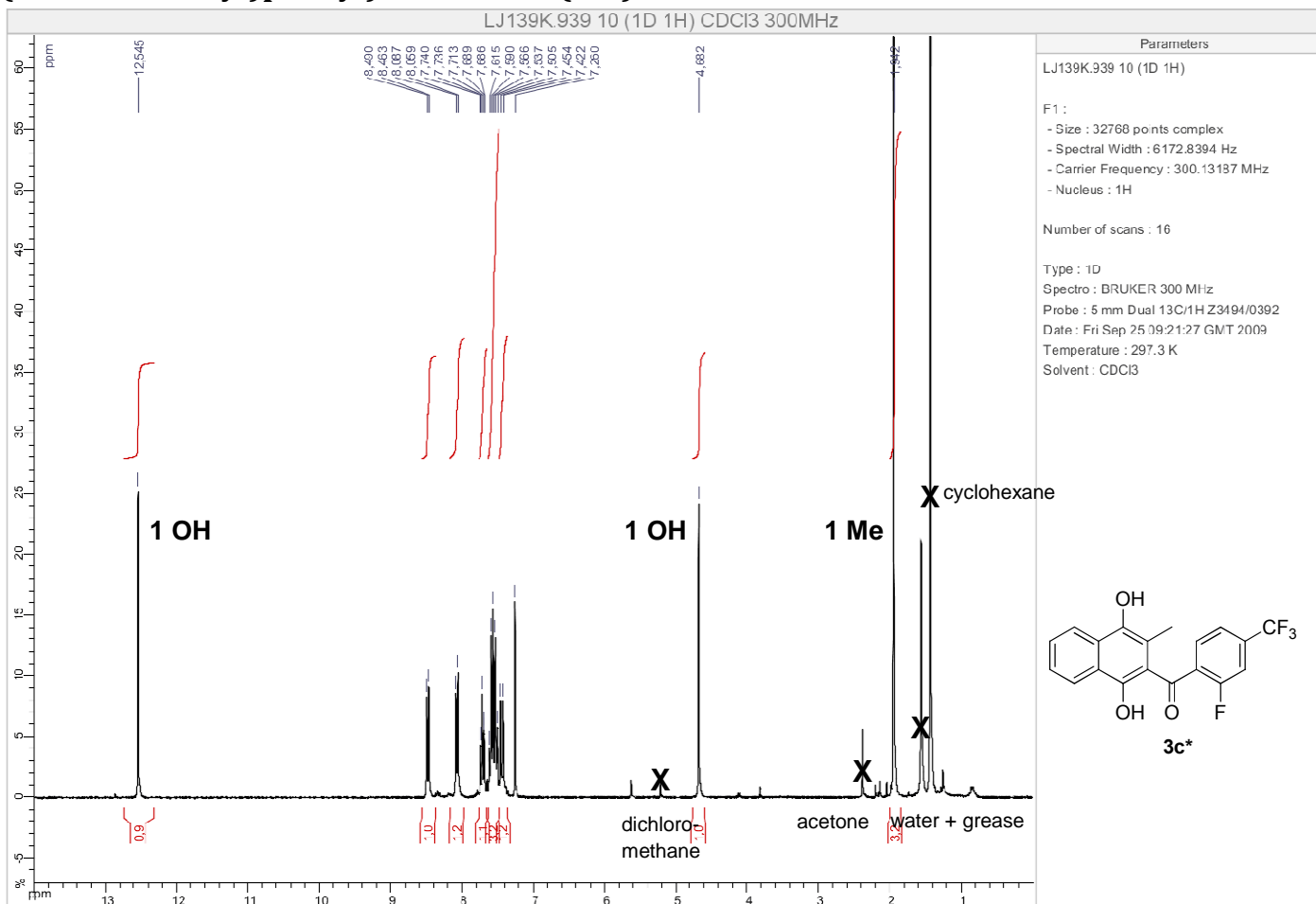




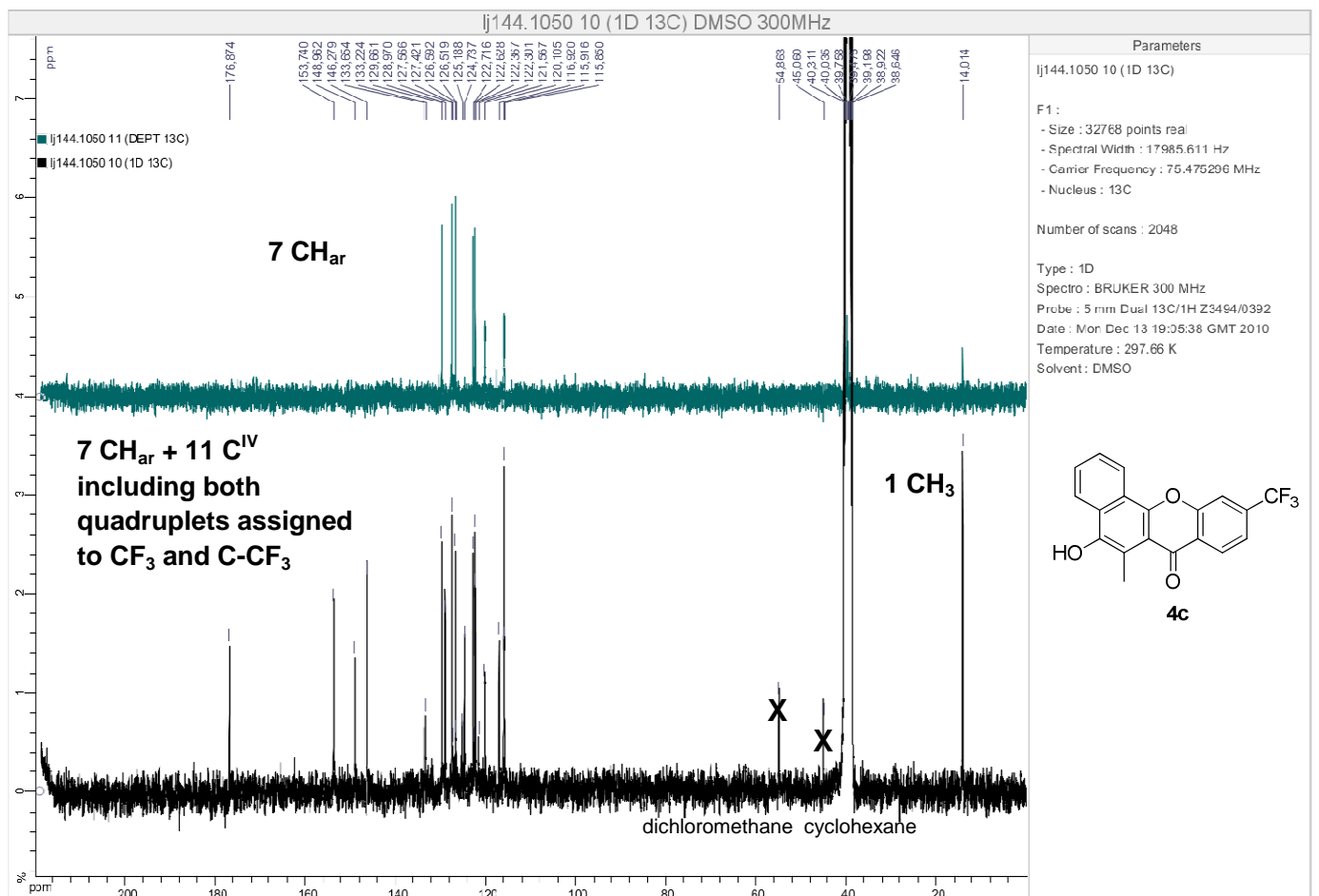
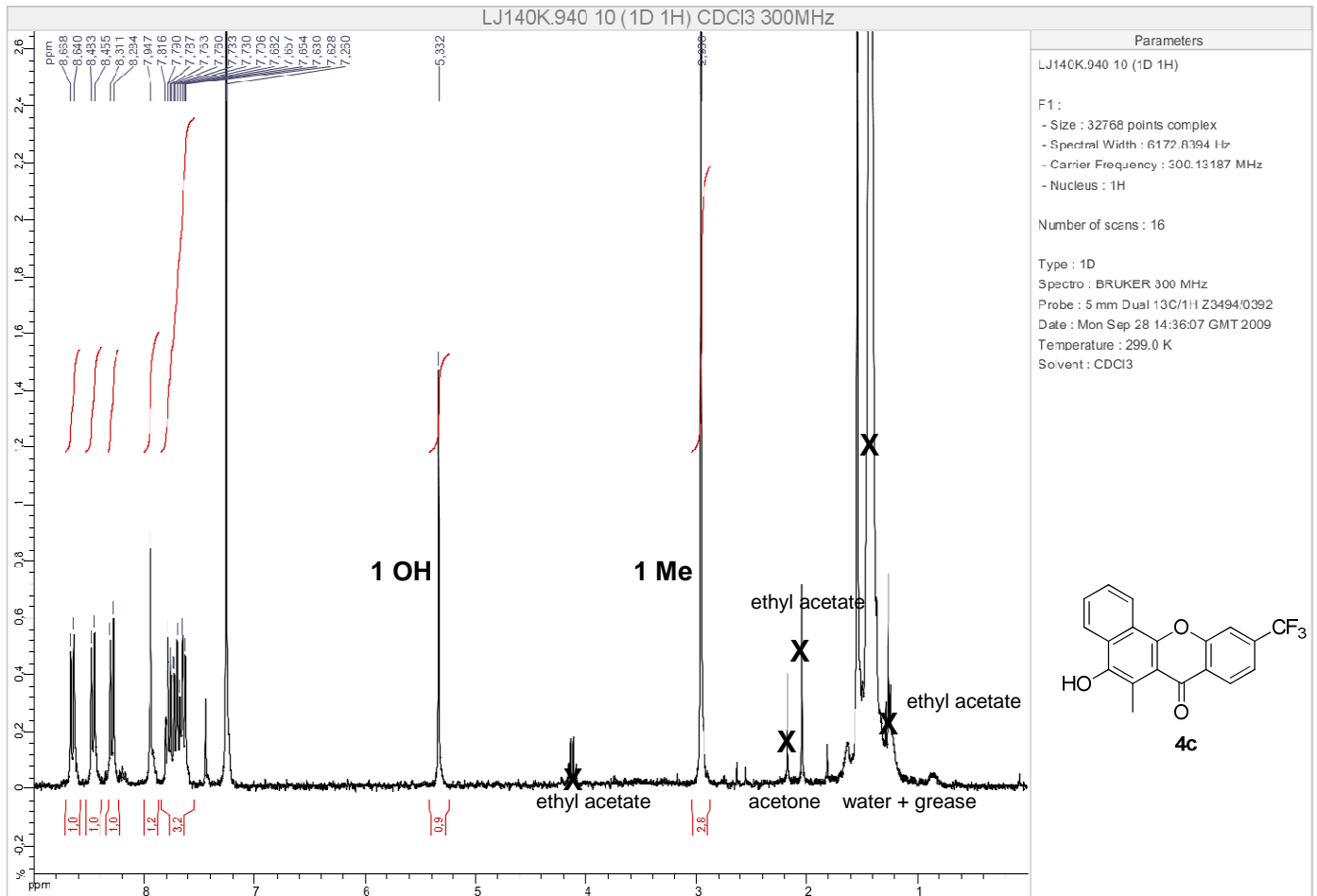
**NMR spectra of 5-methoxy-6-methyl-11-(trifluoromethyl)-7H-benzo[c]xanthen-7-one (7i): zoom of  $^{13}\text{C}$  & DEPT135 spectra.**



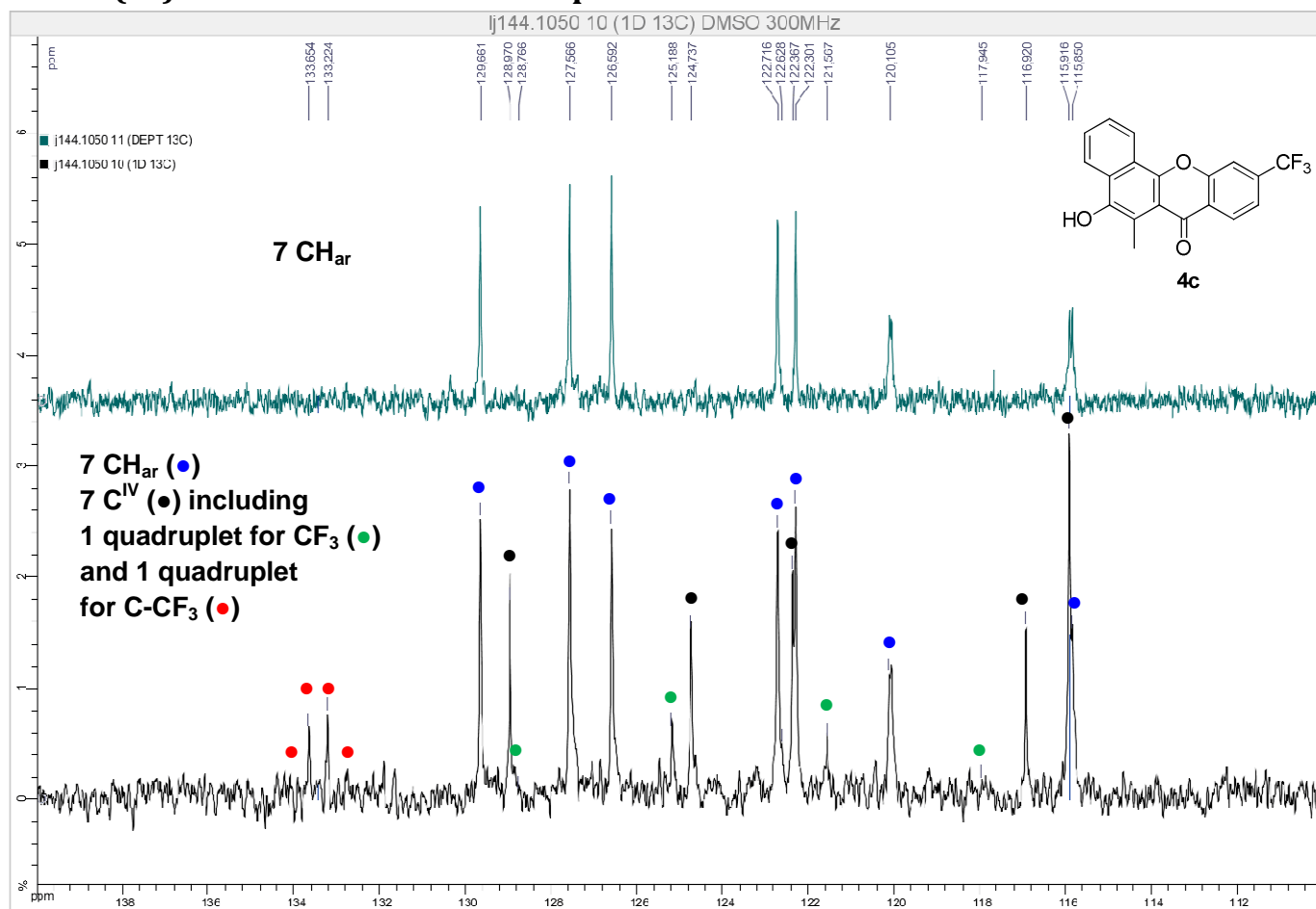
**$^1\text{H}$  and  $^{13}\text{C}$  NMR spectra of (1,4-dihydroxy-3-methylnaphthalen-2-yl)(2-fluoro-4-(trifluoromethyl)phenyl)methanone (**3c\***).**



# NMR spectra of 5-hydroxy-6-methyl-10-(trifluoromethyl)-7H-benzo[c]xanthen-7-one (4c): <sup>1</sup>H spectrum, <sup>13</sup>C & DEPT135 spectra.



**NMR spectra of 5-hydroxy-6-methyl-10-(trifluoromethyl)-7H-benzo[c]xanthen-7-one (4c): zoom of  $^{13}\text{C}$  & DEPT135 spectra.**



# <sup>1</sup>H NMR spectrum of 2-[(4-(trifluoromethyl)phenyl)carbonyl]-4-(methoxymethoxy)-3-methylnaphthalen-1-ol (3c-MOM).

